

Sterically congested quinone methides in photodehydration reactions of 4-hydroxybiphenyl derivatives and investigation of their antiproliferative activity †

Nikola Basarić,^{*a} Nikola Cindro,^a Damir Bobinac,^a Kata Mlinarić-Majerski,^a Lidija Uzelac,^b Marijeta Kralj^b and Peter Wan^{*c}

Received 15th June 2011, Accepted 19th September 2011

DOI: 10.1039/c1pp05182b

In aqueous media, photochemical excitation (S_1) of hydroxyadamantyl, diphenylhydroxymethyl, and hydroxypropyl derivatives of 4-phenylphenol **5–9** leads to solvent-assisted deprotonation of the phenol OH, and protonation of the benzyl alcohol coupled with dehydration, that delivers quinone methides (QMs) **14–18**. The QMs react with CH_3OH converting them in high quantum yields to the photosolvolysis products (overall $\Phi \sim 0.1–0.5$). QMs were characterized by laser flash photolysis in $\text{CH}_3\text{CN–H}_2\text{O}$ and TFE. In TFE, the zwitterionic QM **15** has a lifetime of 250 ns, whereas *para* QMs **16** and **17** have lifetimes of 500 μs and 1.1 s, respectively. Introduction of the steric hindrance to the parent QM structure (with the adamantyl moiety), or additional stabilization by two phenyl rings, results in an increase of QM lifetimes and selectivity in the reactions with nucleophiles. *In vitro* studies of the antiproliferative activity of photochemically generated QMs **15–17** were carried out on one human cancer cell line. Irradiation of cells incubated with **7** showed enhanced antiproliferative activity compared to cells that were not irradiated, in accordance with the activity being due to the formation of QM **16**.

Introduction

Quinone methides (QM) are important intermediates in chemistry and biology.¹ They have attracted considerable interest in the last decades because of their biological activity. It has been demonstrated that QMs react with amino acids² and DNA.³ Particularly interesting is the ability of QMs to alkylate and cross-link DNA,⁴ thus making them potent agents in cancer therapy. For example, the antiproliferative activity of some antibiotics is based on metabolic formation of QMs and subsequent DNA alkylation.⁵ Moreover, Freccero *et al.* have recently investigated DNA alkylation ability of QMs derived from BINOL–amino acid conjugates and the antiproliferative effect of some photogenerated simple BINOL QMs.⁶

QMs can be generated in thermal reactions by oxidation of phenols,⁷ extrusion of water and other small molecules from hydroxybenzyl alcohols,⁸ and fluoride induced desilylation.⁹ More appealing methods, however, rely on the use of milder approaches,¹⁰ primarily photochemical.¹¹ QMs can be formed in photochemical reactions from suitably substituted phenols with appropriate benzylic moieties, such as benzyl alcohols,¹² benzylacetates,¹³ or benzylamines.^{2,14}

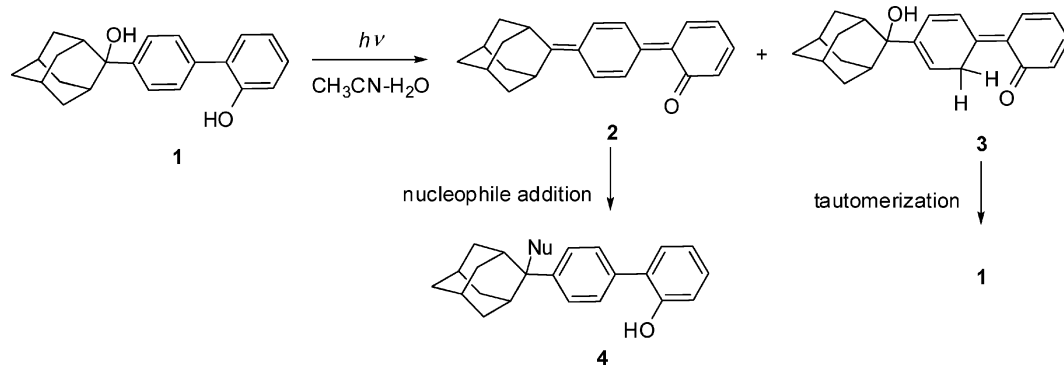
Recently we reported on the photochemical formation of long-lived QMs in these systems that were further substituted by bulky polycyclic adamantyl groups.¹⁵ The bulkiness of the adamantyl polycycle sterically hindered attack of nucleophiles to the methylene position of the QMs, making them longer-lived and more selective towards N-nucleophiles, which is a highly desirable property for use in biological (aqueous) systems as a DNA alkylating agent. The other approach to achieve selectivity in targeting biological nucleophiles, including DNA, is by conjugation of the QM to a selective ligand, such as naphthalene diimide.¹⁶ In continuation of the research we prepared a series of adamantyl-substituted 2-hydroxybiphenyls wherein we observed competition of two photochemical pathways from their singlet excited state.¹⁷ For example, due to an increased acidity of the phenolic OH in the singlet excited state, 2-hydroxybiphenyl derivative **1** underwent ES IPT (excited state intramolecular proton transfer), and solvent-assisted dehydration, both processes giving rise to QMs. QM **2** that was formed by dehydration, reacted with nucleophiles

^aDepartment of Organic Chemistry and Biochemistry, Ruđer Bošković Institute, Bijenička cesta 54, 10 000, Zagreb, Croatia. E-mail: nbasari@irb.hr; Fax: 385 1 4680 195; Tel: 385 12 4561 141

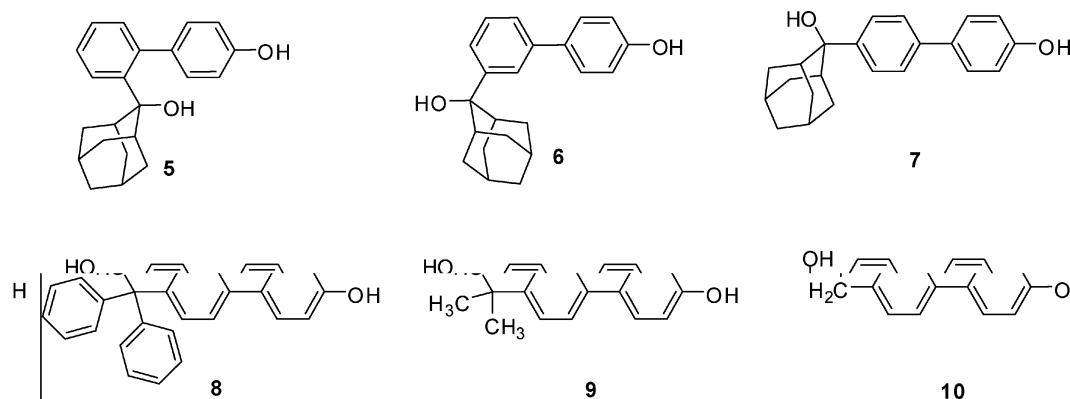
^bDepartment of Molecular Medicine, Ruđer Bošković Institute, Bijenička cesta 54, 10 000, Zagreb, Croatia

^cDepartment of Chemistry, Box 3065, University of Victoria, Victoria, BC, V8W 3V6, Canada. E-mail: pwan@uvic.ca; Fax: +1 (250) 721-7147; Tel: +1 (250) 721-8976

† Electronic supplementary information (ESI) available: Experimental procedures for the preparation of compounds, UV-vis and fluorescence spectra of compounds **5–9**, transient absorption spectra obtained by LFP of **5–10**, and ¹H and ¹³C NMR spectra of all prepared compounds. See DOI: 10.1039/c1pp05182b



Scheme 1



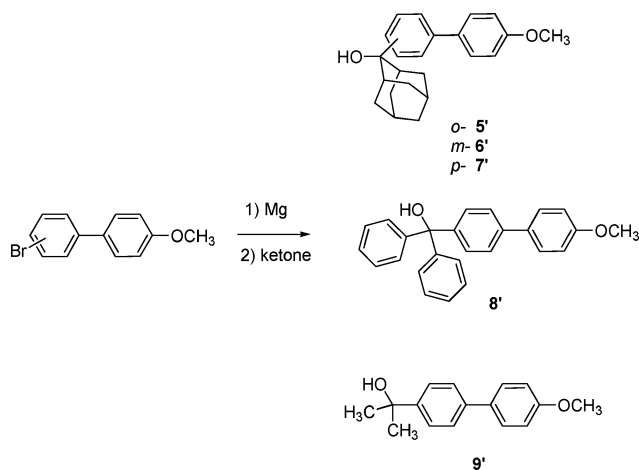
giving adducts **4**, whereas short-lived QM **3** formed by ESIPT, rapidly underwent tautomerization to the starting compound **1** (Scheme 1). QM **2** was detected by laser flash photolysis, giving a transient with a maximum at 430 nm and a band stretching over longer wavelengths, decaying within 1–6 μ s. QM **3** could not be detected by LFP, and its formation was indicated due to the regioselective incorporation of deuterium on photolysis in $\text{CH}_3\text{CN-D}_2\text{O}$.¹⁷

With the aim of finding precursors of QMs that could be used in biological systems, we report herein on the photochemistry of sterically congested 4-hydroxybiphenyl derivatives **5–9**, wherein the above mentioned ESIPT reaction is impossible, and compare their reactivity with the parent 4-hydroxybiphenyl **10**. On excitation, the investigated compounds are expected to undergo only photosolvolytic, giving rise to QMs that would be long-lived and selective in reactions with nucleophiles. Therefore, we performed preparative photolyses in the nucleophilic solvent (CH_3OH) and carried out characterization of the compounds by fluorescence spectroscopy and laser flash photolysis. We also investigated if solvent assisted photochemical deuterium incorporation takes place in the biphenyls **6** and **7**, and fluorene **11**, to probe for the possibility of solvent assisted formal proton transfer from the phenol to the carbon atoms that would decrease quantum yields in photodehydration reactions. In addition, we performed a preliminary *in vitro* antiproliferative study with the photochemically generated QMs on a colon cancer cell line HCT 116 and showed that the irradiation of cells incubated with **7** leads to an enhanced antiproliferative effect compared to cells that were kept in dark.

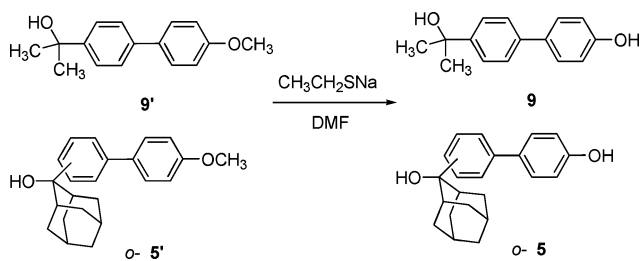
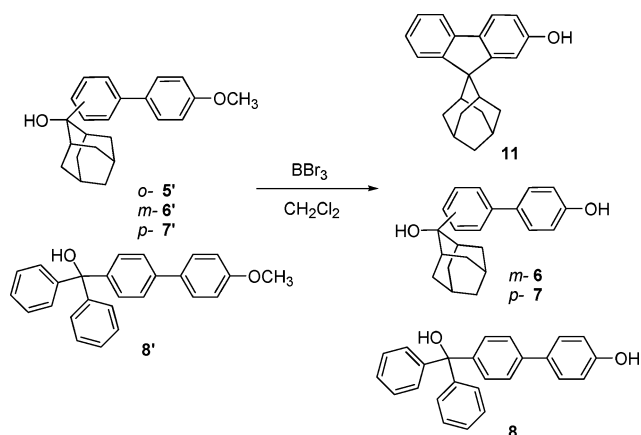
Results and discussion

Synthesis

The 4-hydroxybiphenyls **5–9** were prepared by modifying a published procedure.¹⁵ The synthetic sequence involved a Suzuki reaction for the preparation of bromo-substituted 4-methoxybiphenyls, which were transformed by Grignard reactions to the corresponding methoxy derivatives **5'–9'** (Schemes 2–4). Subsequent reaction with a Lewis acid, BBr_3 , gave rise to **6–8** and **11**, whereas **5** and **9** were prepared under basic conditions



Scheme 2



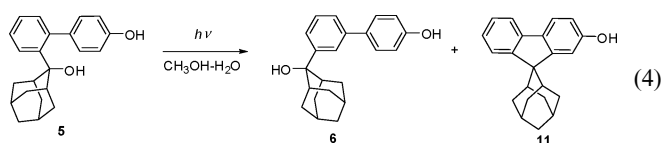
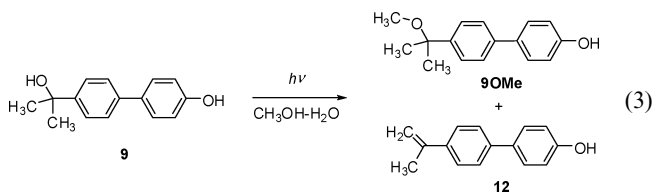
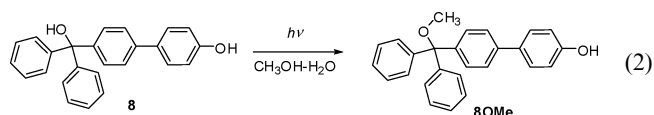
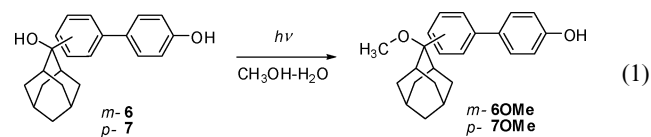
by cleavage of the ether by sodium thiolate according to the modification of a published procedure.¹⁸

Preparative irradiations

The photochemical reactivity of biphenyls **5–8** and their ability to form stable products was first analyzed by irradiations in CH_3CN or $\text{CH}_3\text{OH}-\text{H}_2\text{O}$ (1 : 1) solutions at 254 nm in UV-vis cuvettes. After each short exposure to light, the UV-vis spectra were taken. The experiments for the *ortho* derivative **5** indicated formation of a new species that had absorption maxima at longer wavelengths, and the conversion was more efficient in the presence of H_2O (see supporting info†). On the other hand, experiments with **6–8** indicated no change at shorter irradiation times, whereas on prolonged irradiation disappearance of the absorption bands at 270 nm and formation of broader bands were observed, indicating decomposition. However, the decomposition process was much slower in the presence of H_2O (For example of **7**, see the supporting info†).

To probe for the photodehydration reactions that would give QMs from **5–9**, we performed irradiations in the presence of the nucleophilic solvent CH_3OH , wherein photosolvolytic (*viz.* substitution of the hydroxyl group by methoxy, or photomethanolysis) would be an indication of the QM formation, as shown in previous reports.^{12,15,17,19} The preparative irradiations were performed at 254 nm in CH_3OH and $\text{CH}_3\text{OH}-\text{H}_2\text{O}$ solutions with different H_2O content. The course of the photochemical reaction was followed by HPLC. Control experiments were performed where the solutions were kept in the dark to check for the possibility of the thermal methanolysis reactions. Thermal methanolysis was observed for **7**; however, it was significantly slower compared to the photochemical reaction. Conversion to the photoproducts

was cleaner and more efficient in aqueous mixtures containing more than 10% H_2O (see supporting info†), in agreement with the above described irradiations in UV-vis cuvettes and a higher probability of transferring a proton from the excited phenol to the clusters of H_2O than CH_3OH .²⁰ In aqueous CH_3OH solutions the photolysis of **6–8** gave only photomethanolysis products **6OMe–8OMe**, respectively (eqn (1) and (2)), that were formed in high yields upon longer irradiation times (16 lamps, 15 min–1 h, yields 50–100%). On the other hand, the dimethyl derivative **9** gave two products, the methanolysis product **9OMe** and the vinyl derivative **12**, in a ratio 1 : 1. Irradiation of **5** gave fluorene **11** and, surprisingly, underwent phototransposition to furnish the *meta* derivative **6** (eqn (4)), that was, on prolonged irradiation, converted to the methoxy derivative **6OMe**. Since fluorene **11** and the *meta* derivative **6** absorb light at longer wavelengths than **5**, the analytical UV-vis experiments indicated their formation (*vide supra*). The photochemical products were isolated after photolyses by preparative TLC or crystallization wherein they were separated from the unreacted starting compounds and some unidentified high molecular weight material.



Formation of the methanolysis products from **6–9** suggested the presence of QM intermediates in their photochemistry. However, the photomethanolysis can in principle also take place *via* cationic intermediates. In that case, the photolysis of the methoxy derivatives **6'–9'** would also give rise to the methanolysis products. Hence, we photolyzed **6'–9'** to check if the methanolysis products can be formed with similar quantum efficiencies. However, irradiations under the same conditions as for **6–9** gave no observable methanolysis products, only the starting materials were recovered. Prolonged irradiations, on the other hand, gave rise to the traces of the photomethanolysis products (according to NMR of the crude irradiation mixtures) that were formed in significantly lower quantum yields.

According to previous reports, the QMs are formed in a solvent-assisted proton transfer in the singlet excited state from the acidic phenolic OH to the benzyl alcohol, coupled by dehydration.^{12,15,17,19} Hence, the efficiency of QM formation and the subsequent

Table 1 Quantum yields of the photomethanolysis reaction^a

Comp.	Φ
5	0.13 ± 0.03^b
6	0.4 ± 0.1
7	0.11 ± 0.03
8	0.5 ± 0.2
9	0.05 ± 0.03
10	0.026^c

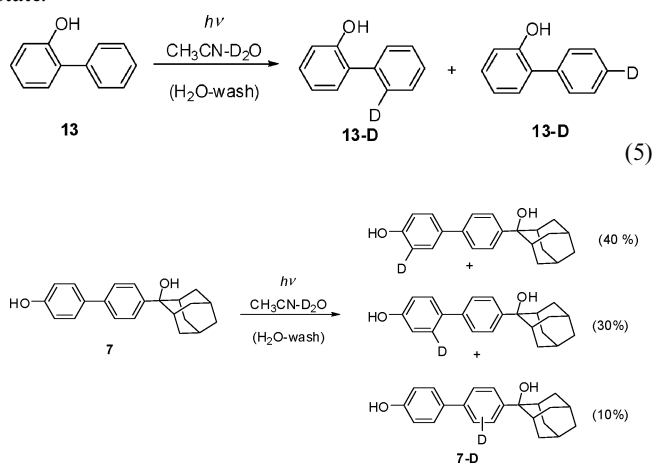
^a Photolysis performed in CH₃OH–H₂O (1 : 1) by use of two actinometers: photolysis of 2-hydroxybenzyl alcohol in CH₃OH–H₂O ($\Phi = 0.23$),¹² and photolysis of valerophenone in aqueous CH₃CN ($\Phi = 0.65 \pm 0.03$).²¹ The composition of the solution was analyzed by HPLC. ^b Quantum yield for the formation of **11** and **6OMe**. ^c Taken from the literature.^{19b}

photomethanolysis should depend on the pH of the solution.^{19a} Therefore, we performed irradiations of **6** and **7** in CH₃OH–H₂O (20%) at different pH (2.4–10.1) and analyzed the composition of the solution by HPLC (see supporting info†). The change of the solution pH in the range 4–8 had no effect to the efficiency of the formation of **6OMe** and **7OMe**, whereas at pH 10, some weak base catalysis was observed. Interestingly, at pH 2.4, a significant acid catalysis was observed for the formation of **7OMe**, whereas acid had no effect to the formation of **6OMe**. The observation parallels the reactivity of the anticipated corresponding QMs, and is in accordance with the pH-dependant reactivity of QMs in hydration reactions.¹³

Quantum yields for the photochemical transformations of **5–9** were measured by use of two actinometers: photomethanolysis of 2-hydroxybenzyl alcohol in CH₃OH–H₂O ($\Phi = 0.23$),¹² and by use of a primary actinometer, photolysis of valerophenone giving acetophenone in aqueous CH₃CN ($\Phi = 0.65 \pm 0.03$).²¹ The absorbances of the solutions were measured prior to irradiations, whereas the composition of the irradiated solution was analyzed by HPLC. Measurements were performed in triplicate and the mean values are reported (Table 1). The efficiency of the photomethanolysis of the biphenyl derivative **8** was very much dependant on the CH₃OH supplier. Hence, the measured quantum yield was difficult to reproduce and the reported value contains a large error. As can be seen from the data, substitution of the parent molecule with methyl groups increased quantum yield of the methanolysis 2 times, whereas incorporation of the adamantyl moiety increased quantum yield 5 times. The observed quantum yields of the photomethanolysis are also in agreement with the well-known *meta* effect in photochemistry,²² since the *meta* derivative **6** shows an about 4 times higher quantum yield than the corresponding *para* derivative **7**.

Irradiation of 2-phenylphenol (**13**) in the presence of a large amount of D₂O gives rise to the ESIPT from the phenol and deuterium incorporation at the carbon atom at the 2' (*ortho*) position of the adjacent phenyl ring, as well as to a solvent assisted ESPT and deuterium incorporation at the 4' (*para*) position of the biphenyl (giving **13-D**, eqn (5)).²³ In the biphenyl systems **5–9** the ESIPT from the phenol to the adjacent phenyl ring is not possible since the phenol is not in proximity to the adjacent phenyl ring. However, the question remains if the ESPT assisted by solvent could lead to deuterium incorporation, as is the case in the parent system at the 4' position. Therefore, we carried out photolyses (16 lamps, 1 h) of **6**, **7** and **11** in CH₃CN–D₂O (10%). After photolyses, a large excess of H₂O was added

to replace the phenolic OD by OH and the extractions with CH₂Cl₂ were carried out. The photolysis mixtures were analyzed by NMR and MS to investigate the position and the extent of deuterium incorporation, respectively. Photolysis of **6** and **7** gave rise to deuterium incorporation at the biphenyl moiety (MS indicated 10% of the deuterated species), whereas no deuterium incorporation was observed on photolysis of fluorene **11**. However, deuterium was not incorporated regiospecifically, as in the case of 2-hydroxybiphenyl. The NMR spectra indicated that deuterium mostly entered at the phenol ring (not at the adjacent phenyl ring, Scheme 5), in agreement with some minor deuteration pathways (presumably *via* radicals or radical-cations) and not *via* the excited state proton transfer. The non-observation of the regiospecific deuterium incorporation in the adjacent phenyl ring is in agreement with the lower acidity of 4-phenylphenols (compared to 2-phenylphenols) and the lower extent of charge transfer from the phenol to the adjacent ring in the singlet excited state.²⁴

**Scheme 5**

Fluorescence study

It is well-accepted that proton transfer reactions and formation of QMs from phenols take place from the singlet excited state.^{12,19} Hence, we studied the fluorescence of **5–9** to get more insight into their singlet state reactivity. In CH₃CN solutions, **6–8** showed strong fluorescence with maxima at ~330 nm, whereas the *ortho* derivative **5** was very weakly fluorescent. Fluorescence quantum yields were measured by using fluorescence of fluorene in methanol as a reference ($\Phi = 0.68$).²⁵ Lifetimes of the singlet states were measured by time-correlated single photon timing method. The results are compiled in Table 2.

The reported photomethanolysis reaction mechanism involves solvent assisted deprotonation of the phenols due to increased acidity in the singlet excited state, and protonation of the benzyl alcohols coupled by dehydration giving QMs.^{12,15,17,19} Increase of the H₂O content in the CH₃CN solutions of the hydroxybiphenyls **5–9** is thus expected to open a new photochemical pathway, the transfer of the phenolic OH proton to the H₂O clusters, that should give rise to the fluorescence quenching.²⁶ Therefore, in the series of biphenyls **5–9** we probed for the possibility of solvent assisted proton transfer by titrating CH₃CN solutions with H₂O. However, the initial additions of H₂O to the CH₃CN solutions (up to 10 M)

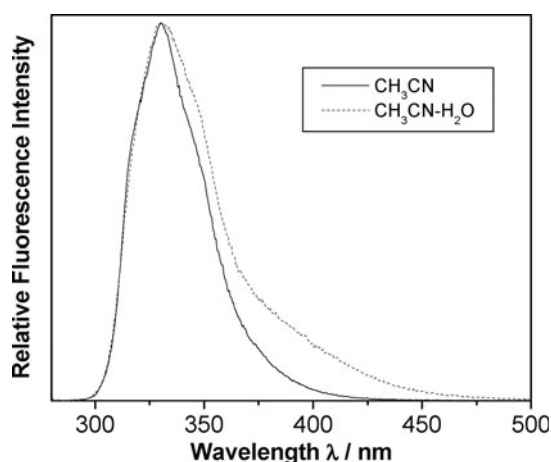
Table 2 Photophysical properties of 4-hydroxybiphenyls **5–9**

	Φ (CH ₃ CN) ^a	Φ (CH ₃ CN-H ₂ O) ^a	τ (CH ₃ CN)/ns ^b	τ (CH ₃ CN-H ₂ O)/ns ^b
5	$\sim 8 \times 10^{-4}$	$\sim 7 \times 10^{-4}$	0.2 ± 0.1 (13%) 7.9 ± 0.1 (77%)	0.2 ± 0.1 (13%) 7.9 ± 0.1 (77%)
6	0.22 ± 0.02	0.18 ± 0.01	8.10 ± 0.05	4.5 ± 0.1 phenol 0.4 ± 0.1 phenolate
7	0.39 ± 0.02	0.44 ± 0.01	7.75 ± 0.05	4.93 ± 0.03 phenol 0.9 ± 0.1 phenolate
8	0.35 ± 0.02	0.34 ± 0.02	7.09 ± 0.01	2.02 ± 0.02 phenol 0.2 ± 0.1 phenolate
9	0.36 ± 0.02	0.30 ± 0.02	10.2 ± 0.1	6.1 ± 0.1 phenol 0.6 ± 0.1 phenolate

^a Quantum yield of fluorescence determined by use of fluorene in CH₃OH as a reference ($\Phi = 0.68$).²⁵ ^b Singlet excited state lifetimes measured by time-correlated single photon timing method.

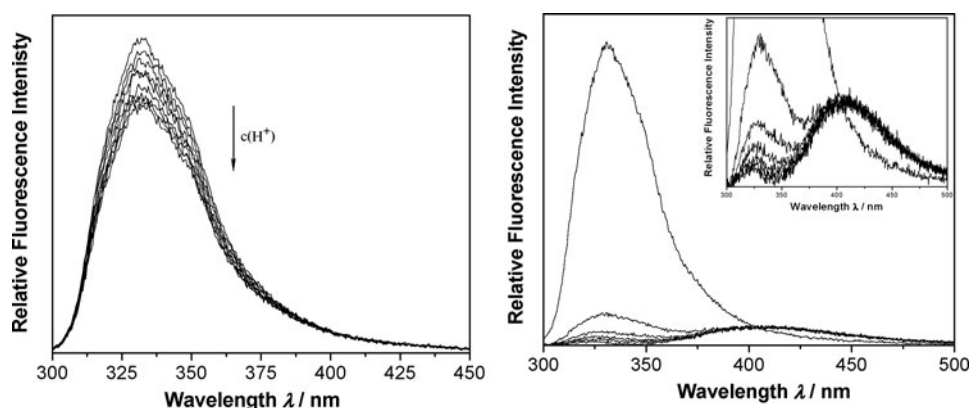
resulted in a weak fluorescence increase, that with further H₂O additions (up to 20 M) leveled off (see the supporting info†). Thus, in CH₃CN-H₂O solution (1 : 4), fluorescence quantum yields of **5–9** were comparable to the yields in neat CH₃CN (Table 2). The increase of the fluorescence on addition of H₂O has already been reported for the adamantyl phenols, that is probably due to the unusual solvation of the very lipophilic adamantyl molecules in aqueous media.¹⁵ However, comparison of the fluorescence spectra of **5–9** in CH₃CN and CH₃CN-H₂O clearly showed a presence of a new shoulder at longer wavelength in the aqueous solvent (for the example of **7**, see Fig. 1). The new band appearing as a shoulder can be attributed to the fluorescence of phenolates that were formed in the singlet excited state due to a proton transfer to the solvent. Fluorescence spectra of **6–9** in basic media (pH > 10) where phenols are deprotonated showed the presence of the same band emitting at longer wavelengths, additionally corroborating the assignment to the phenolate emission (see Fig. 2 and the supporting info†).

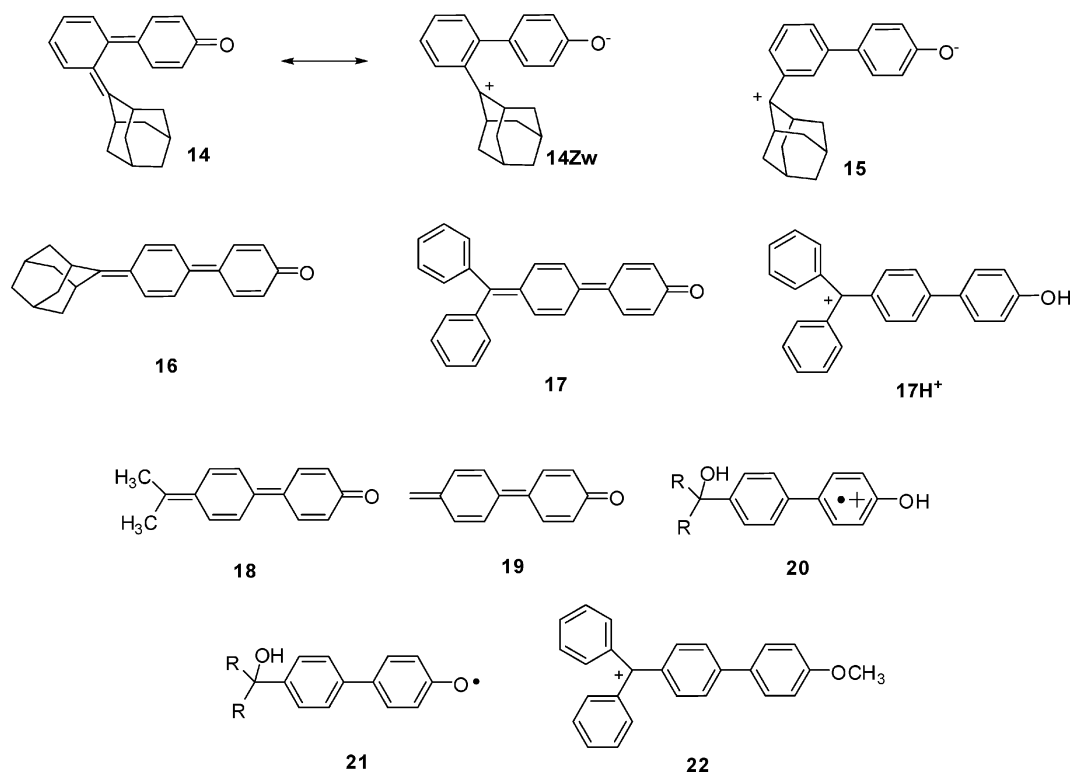
The excited-state proton transfer and formation of phenolates from **6–9** was also indicated by single photon timing (SPT) measurements. Namely, single exponential fluorescence decays of **6–9** in CH₃CN on addition of H₂O became double-exponential. The fluorescence decays in the aqueous media were thus characterized by the presence of a longer-lived decaying component more present at shorter wavelengths, corresponding to phenols. In

**Fig. 1** Normalized fluorescence spectra of **7** in CH₃CN (full line) and CH₃CN-H₂O (1 : 4) (dashed line), $\lambda_{\text{ex}} = 265$ nm.

addition, a shorter-lived decaying component contributing more at longer wavelengths was observed, that was formed during the decay (negative pre-exponential factor), and was attributed to phenolates. It is interesting to note that phenolates exhibit 10 times shorter decay time compared to their corresponding phenols. The finding indicates that phenolates deactivate from the singlet excited state by a nonradiative pathway, presumably *via* a photochemical pathway giving rise to QMs.

The acid–base properties of **6–8** in the aqueous solution in the singlet excited state were further investigated by fluorescence titrations with acid (HClO₄) and base (NaOH). The titrations with acid induced quenching of the fluorescence in the pH range 2.5–3.0. The Stern–Volmer plots (Φ/Φ_0 vs. H⁺ concentration) showed linear relationship, indicating a dynamic quenching. The estimated quenching constants for **6**, **7** and **8** are $k_q = 2 \times 10^{10} \text{ M}^{-1} \text{ s}^{-1}$, $8.6 \times 10^9 \text{ M}^{-1} \text{ s}^{-1}$, and $3.9 \times 10^{10} \text{ M}^{-1} \text{ s}^{-1}$, respectively. It should be mentioned that we observed the fluorescence quenching (without a change of the shape of the fluorescence spectra), and not a fluorescence increase, as would be expected if an increase of the proton concentration blocked the deprotonation of the phenol in the excited state. The finding suggests that the most basic site in the molecule in the singlet excited state is not the phenolate but some other site, presumably the benzyl alcohol moiety. Indeed, the estimated $\text{p}K_a$ value in the excited state of 4-phenylphenol is 1.83

**Fig. 2** Quenching of the fluorescence of **6** in CH₃CN-H₂O (1 : 4) with HClO₄ (left, concentration range 0–0.0025 M) and NaOH (right, concentration range 0–0.012 M).



± 0.04 ,²⁷ so a higher concentration of acid (than in the pH range 2.5–3) would be required to block the deprotonation of the phenol in the excited state. Fluorescence titration with acid, furthermore, suggests that in the excited state proton transfer assisted by solvent from the phenol to the benzyl alcohol can take place. Titration with base also induced fluorescence quenching. However, in addition to the quenching, a significant change of the fluorescence spectra was observed. The band with a maximum at 330 nm corresponding to the phenol gradually disappeared and only a much weaker band at 430 nm corresponding to the phenolate was observed. The finding additionally corroborates the assignment of the observed shoulder in the fluorescence spectrum in $\text{CH}_3\text{CN-H}_2\text{O}$ (1 : 4) to the phenolate emission.

Laser flash photolysis (LFP)

To characterize QMs and other possible long-lived intermediates in the photochemistry of biphenyls **5–10**, we carried out LFP experiments. Since the formation of QMs from **5–10** is anticipated only in aqueous media, the transient spectra were recorded in N_2 and O_2 -purged CH_3CN and $\text{CH}_3\text{CN-H}_2\text{O}$ (1 : 1) solutions, wherein the difference in the observed transients in these two solvent systems could in principle be due to QMs or other intermediates formed by proton transfer reactions.

In the N_2 - and O_2 -purged $\text{CH}_3\text{CN-H}_2\text{O}$ solutions of **5** we observed transients with the maximum at 350 nm and ~700 nm, that decayed with the rate constant $k \sim 3\text{--}5 \times 10^4 \text{ s}^{-1}$ ($\tau \sim 20\text{--}30 \mu\text{s}$) and which were not affected by O_2 (see supporting info†). However, we could not assign the observed transient absorption to QM intermediate **14**. Due to a steric hindrance of the adamantyl moiety, **14** should probably be better represented as a zwitterion **14Zw**, which is expected to be shorter-lived in $\text{CH}_3\text{CN-H}_2\text{O}$ solution than the

observed transient. Hence, no assignment of the transient was made.

The transient spectra of **6**, **7**, **9** and **10** in CH_3CN solutions were similar. In the N_2 -purged CH_3CN solution (and $\text{CH}_3\text{CN-H}_2\text{O}$) we observed a strong transient absorption with a maximum at 390 nm, and a weak shoulder stretching over the whole visible wavelength region. Its decay was bi-exponential ($\tau \sim 1 \mu\text{s}$, $k \sim 1.0 \times 10^6 \text{ s}^{-1}$, and $\tau \sim 10 \mu\text{s}$, $k \sim 1 \times 10^5 \text{ s}^{-1}$), and it was strongly quenched by O_2 (in O_2 -purged solution, $\tau \sim 30\text{--}200 \text{ ns}$, $k \sim 5.0 \times 10^6\text{--}3.3 \times 10^7 \text{ s}^{-1}$). Due to the strong quenching by O_2 , and in accordance with the transient spectra of similar phenylphenols,^{17,19,23} we assigned the observed transients to the corresponding triplet excited states of **6**, **7**, **9** or **10**. In the O_2 -purged CH_3CN solutions, after the decay of the triplet, the short-lived transients were observed with absorptions at 600–700 nm ($\tau \sim 20 \text{ ns}$, $k \sim 4.9 \times 10^7 \text{ s}^{-1}$ and $\tau \sim 200 \text{ ns}$, $k \sim 5 \times 10^6 \text{ s}^{-1}$), and longer-lived transients absorbing at 370 nm, and at 500–600 nm ($10\text{--}20 \mu\text{s}$, $k \sim 10^3\text{--}5 \times 10^4 \text{ s}^{-1}$, and $100 \mu\text{s}$, $k \sim 1 \times 10^2 \text{ s}^{-1}$), that were not affected by O_2 or N_2O . Hence, the transients are not due to triplets or solvated electron. Moreover, for O_2 -purged CH_3CN solution of **7**, a rise of the transient absorption at 550–570 nm was observed that followed the same kinetics as the decay of the transient at $>600 \text{ nm}$ ($\tau \sim 240 \text{ ns}$, $k \sim 4.2 \times 10^6 \text{ s}^{-1}$). By comparison to the published transient spectra of aryl radical-cations²⁸ and phenoxy radicals,²⁹ these transient absorptions were assigned to the corresponding radical-cations **20** (at 600–700 nm) formed by photoionization, and the phenoxy radicals **21** (500–600 nm), that were formed by deprotonation of the corresponding radical-cations. The radical-cations are formed by one-photon ionization since we observed a linear dependence of the intensity of the signal with the laser power.

The transient absorption spectra in O_2 -purged $\text{CH}_3\text{CN-H}_2\text{O}$ solution of **7**, **9** and **10** were more complex than the corresponding spectra in CH_3CN solution (see supporting info†), in accordance

with the formation of new transients from the photochemical proton transfer pathways. However, transient absorption spectra of **6** in O₂-purged CH₃CN–H₂O gave no transient absorption that could be assigned to the presence of the zwitterionic QM **15**. This zwitterion has a dialkylbenzyl cation as a chromophore, so its absorption is expected in the 350–400 nm region.³⁰ In the aqueous system it should be characterized by a very short lifetime <20 ns that cannot be detected on our LFP system. In the transient spectra of O₂-purged CH₃CN–H₂O solutions of **7**, **9** and **10**, in the wavelength region at ~350 nm, and at 500–600 nm, in addition to the above mentioned transient absorptions corresponding to the phenoxyl radicals, more persistent species were detected that we tentatively assigned to the corresponding QMs **16**, **18**, and **19**, respectively. They decayed in 100 μs–0.5 ms, but due to their weak intensity it was difficult to precisely estimate their decay kinetics, and perform the quenching study. Nevertheless, substituted biphenyl QMs **16** and **18** showed slower decay kinetics than the parent biphenyl QM **19** ($\tau \sim 67 \mu\text{s}$, $k = 1.5 \times 10^4 \text{ s}^{-1}$).^{19b} The observed shorter lifetimes than for the monophenyl *o*- and *p*-quinone methides (2–4 ms, and 0.3 s, respectively)^{2,13} are due to a loss of aromaticity of two phenyl rings in the biphenyl QMs, compared to only one in the parent monophenyl QM structure.

It is known that QMs and cations display longer lifetimes in polar and non-nucleophilic solvents like trifluoroethanol (TFE).^{12,15,19,30} Therefore, we performed LFP study of **6** and **7** in TFE. In the transient absorption spectra of O₂-purged solution of **6** in TFE, besides the transients described above corresponding to the radical-cation and the phenoxyl radical, we observed a transient at 380–390 nm that decayed with a rate constant $k \sim 4.0 \times 10^6 \text{ s}^{-1}$ ($\tau \sim 250 \text{ ns}$). The transient was quenched by nucleophiles CH₃OH and ethanolamine with the rate constants $k_q = 3 \times 10^7 \text{ s}^{-1} \text{ M}^{-1}$ and $k_q = 2 \times 10^8 \text{ s}^{-1} \text{ M}^{-1}$, respectively, so we assign it to the zwitterion **15**. The transient could, in principle, be due to the corresponding cation, but the benzyl cation would probably be shorter-lived than the zwitterion, and hence not detectable by the nanosecond LFP. Namely, phenoxide (O⁻) in the *meta* position has an electron donating character (Hammett constant $\sigma_m = -0.47$), whereas OH in the *meta* position has electron withdrawing character ($\sigma_m = 0.12$).²⁵ Although phenoxide in **15** is not at the same ring as the cation, some stabilization is expected through conjugation.

In O₂-purged TFE solution of **7**, the transient was observed at 650–750 nm ($\tau \sim 35 \text{ ns}$, $k \sim 2.8 \times 10^7 \text{ s}^{-1}$, and $\tau \sim 800 \text{ ns}$, $k \sim 1.2 \times 10^6 \text{ s}^{-1}$) corresponding to radical-cation **20**. It was quenched by CH₃OH and ethanolamine with the rate constants $k_q = 3\text{--}4 \times 10^7 \text{ s}^{-1} \text{ M}^{-1}$ and $k_q > 5 \times 10^9 \text{ s}^{-1} \text{ M}^{-1}$, respectively. At 500–650 nm, a more persistent transient absorption was observed that decayed with the rate constants $k \sim 1 \times 10^4 \text{ s}^{-1}$ ($\tau \sim 100 \mu\text{s}$), and $k \sim 2 \times 10^3 \text{ s}^{-1}$ ($\tau \sim 500 \mu\text{s}$). The longer-lived transient with the lifetime of 500 μs was assigned to QM **16**. The transient was quenched by CH₃OH and ethanolamine with the rate constants $k_q = 3 \times 10^4 \text{ s}^{-1} \text{ M}^{-1}$ and $k_q = 2 \times 10^4 \text{ s}^{-1} \text{ M}^{-1}$, respectively. However, the estimated quenching constant probably represents only a lower limit, since the quencher also reacts with the transient radical-cations.

The transient absorption spectra of **8** were different from those described above. In N₂-purged CH₃CN solution, a strong transient absorption was observed with a maximum at 400 nm that decayed with a bi-exponential law with $k \sim 8.3 \times 10^5 \text{ s}^{-1}$ ($\tau \sim 1.2 \mu\text{s}$), and $k \sim 8.3 \times 10^4 \text{ s}^{-1}$ ($\tau \sim 12 \mu\text{s}$). It was quenched by O₂, so we assigned

Table 3 Bimolecular quenching constants for QM **17** and cation **22** in TFE solution

Transient species	CH ₃ OH $k_q/\text{s}^{-1} \text{ M}^{-1}$	Ethanolamine $k_q/\text{s}^{-1} \text{ M}^{-1}$
17	3.6	4.0×10^3
22	4.9×10^3	5.9×10^4

it to the triplet state of **8**. In addition, transient absorptions were observed with a broad band at 400–500 nm decaying with $k \sim 1.0 \times 10^4 \text{ s}^{-1}$ (100 μs), which in analogy to previous transients we assigned to the phenoxyl radical **21**. Addition of H₂O to the CH₃CN solution changed the appearance of the transient absorption spectra. A new broad band appeared at 500–700 nm with a maximum at 580 nm (Fig. 3). The transient was not quenched by O₂. In O₂-purged CH₃CN–H₂O (1 : 1) the decay of the transient absorption was bi-exponential with $k \sim 1.0 \times 10^4 \text{ s}^{-1}$ (100 μs) and $k \sim 8.3 \times 10^2 \text{ s}^{-1}$ ($\tau \sim 1.2 \text{ ms}$). The longer-lived transient that is formed only in the aqueous media ($\tau \sim 1.2 \text{ ms}$) could in principle be due to QM **17**, or cation **17H**⁺. However we assigned it to the QM since triarylmethyl cations in aqueous media decay faster (for trityl cation $k = 1.5 \times 10^5 \text{ s}^{-1}$).³¹ In addition, we performed quenching with sodium azide, an ubiquitous cation quencher and observed slower quenching kinetics ($k_q = 1.2 \times 10^6 \text{ s}^{-1} \text{ M}^{-1}$) than reported for the triarylmethyl cations (for trityl cation $k_q = 9.4 \times 10^9 \text{ s}^{-1} \text{ M}^{-1}$).³²

LFP of TFE solution of **8** and **8'** was performed to characterize QM **17** and cation **22** (Fig. 4). In O₂-purged TFE solutions of **8** and **8'**, similar transient absorption spectra were observed with maxima at 390 and 580 nm, in accordance with the similar structure of both chromophores. However, in the spectra of **8**, an additional transient absorption band was present at >650 nm. The transients in O₂-purged TFE solution at 500–600 nm for both compounds decayed with similar bi-exponential kinetics that were not affected by O₂, $k \sim 2.3 \times 10^3 \text{ s}^{-1}$ ($\tau \sim 430 \mu\text{s}$) and $k \sim 0.9 \text{ s}^{-1}$ ($\tau \sim 1.1 \text{ s}$) for **8**, and $k \sim 2\text{--}10 \times 10^3 \text{ s}^{-1}$ ($\tau \sim 100\text{--}500 \mu\text{s}$), $k = 1.15 \text{ s}^{-1}$ ($\tau \sim 0.9 \text{ s}$) for **8'**. Similar decay kinetics for both compounds suggested that we detected the same type of transient species from both compounds, the cation. However, quenching experiments with nucleophiles CH₃OH and ethanolamine revealed very different quenching kinetics (Table 3) in accordance with the different nature of the transient species. Consequently, long-lived transients with lifetimes of 1.1 s, and 0.9 s we assigned to QM **17** and cation **22**, respectively.

Photochemical reaction mechanisms

From the results of preparative photolyses as well as fluorescence and LFP studies, the mechanisms of photochemical reactions of **5–9** can be proposed. Upon excitation of **5**, one of the deactivation channels from the singlet excited state leads to the phototransposition product **6**. The phototransposition is a well-known reaction for polyalkylated benzene derivatives, particularly with bulky substituents.³³ Our finding is in accordance with a deactivation pathway giving rise to overall phototransposition generating **6** in the ground state. However, to the best of our knowledge the phototransposition has not been reported for phenols. Furthermore, our finding suggests that the excitation of **5** resides more on the adjacent phenyl ring than at the phenol,

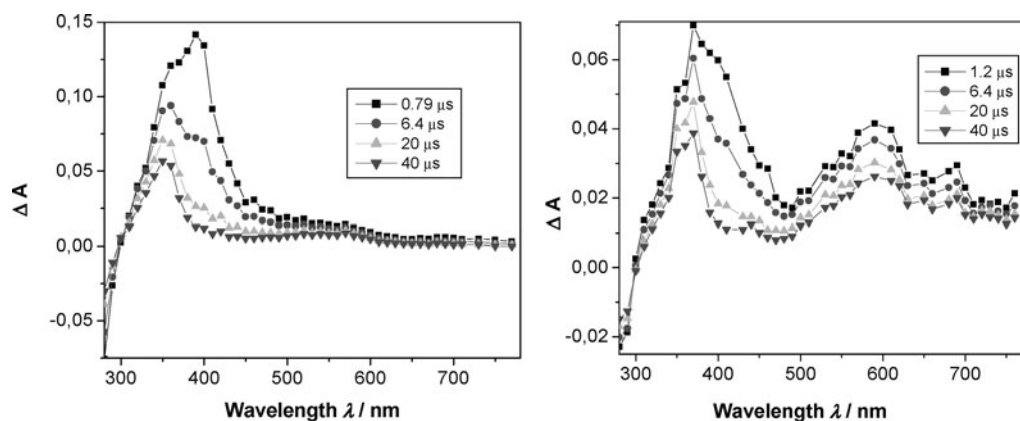


Fig. 3 Transient absorption spectra in N_2 -purged solution of **8** in CH_3CN (left) and $\text{CH}_3\text{CN}-\text{H}_2\text{O}$ (right).

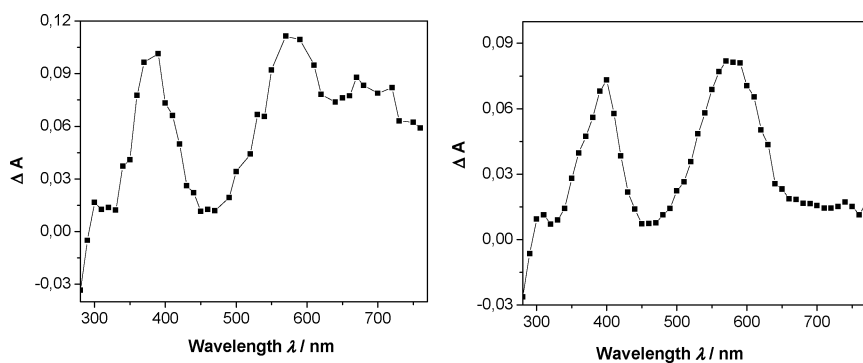


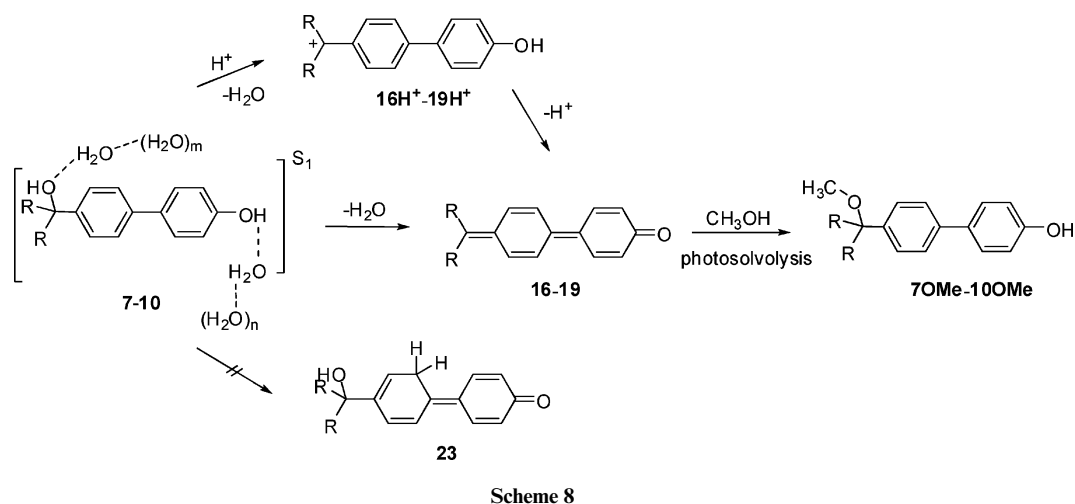
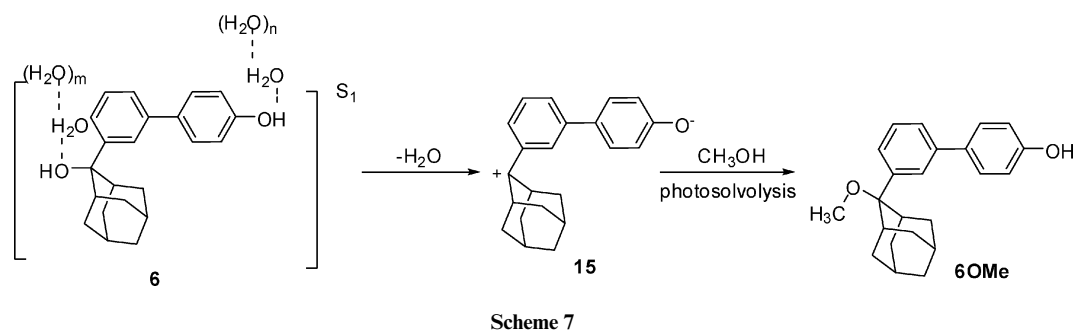
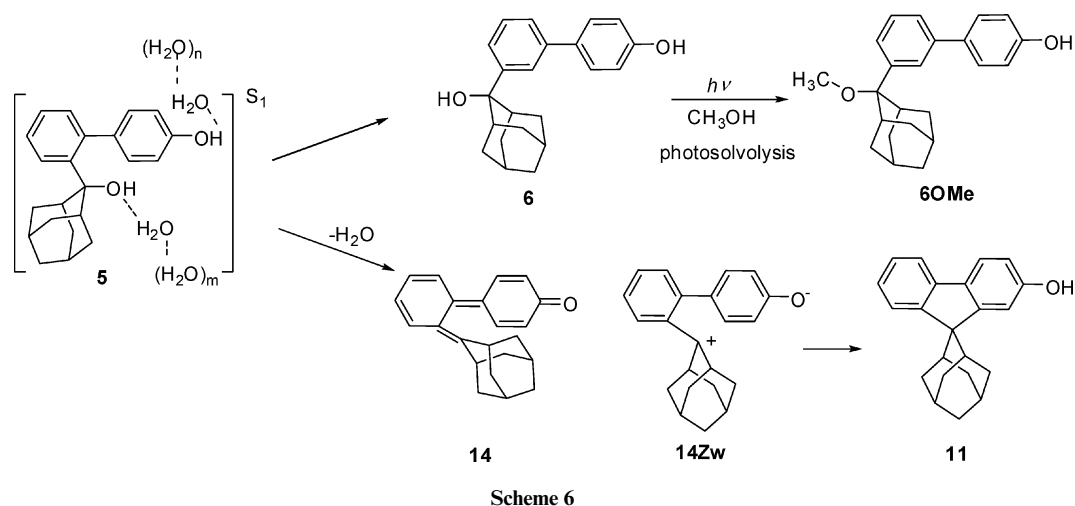
Fig. 4 Transient absorption spectra in O_2 -purged TFE solution of **8** 180 ns after the laser pulse (left) and **8'** 1.6 μs after the laser pulse (right).

which can also be deduced from the UV-vis spectrum wherein the maximum is significantly hypsochromically shifted compared to the spectra of **6** and **7**. In addition, the deactivation of the singlet excited state giving rise to phototransposition results in low fluorescence of **5**. Besides phototransposition, an important photochemical pathway from the singlet excited state in aqueous solvent involves proton transfer from the phenol and formation of the phenolate, as indicated by fluorescence measurements. Formation of the phenolate in the excited state, coupled with solvent assisted protonation of the benzyl alcohol group and dehydration leads to the formation of QM **14**. However, due to the steric hindrance of the adamantane, the QM is probably more represented by its zwitterionic form that very quickly cyclizes to fluorene **11** (Scheme 6). Due to the very fast cyclization, QM **14** has a short lifetime and we were not able to characterize it by LFP. Due to its short lifetime QM **14** does not give photomethanolysis products.

The *meta* derivative **6** is characterized by a significantly higher quantum yield of fluorescence, suggesting that it cannot undergo efficient deexcitation, giving phototransposition as the *ortho* derivative. In the aqueous solvent, the phenol moiety, which becomes more acidic in the S_1 state, undergoes deprotonation, giving phenolate. The excited-state formation of phenolates, coupled with protonation of the benzylic alcohol and dehydration gives rise to zwitterionic QM **15**. The zwitterionic species reacts with nucleophiles giving photosolvolysis products (Scheme 7). Photomethanolysis reaction could principally take place also *via* a cationic intermediate. However, a significantly lower quantum

yield for the photomethanolysis of the methoxy derivative **6'** strongly indicates the importance of the free phenolic OH in the reaction mechanism, and additionally corroborates the mechanistic scenario *via* zwitterion **15**. Zwitterion **15** was detected by LFP in TFE ($\tau \sim 250$ ns).

The important photochemical pathway for the deactivation of the *para* derivatives **7–10** from the singlet excited state involves deprotonation of the phenol, as indicated from the steady-state and time-resolved fluorescence measurements. Formation of phenolates and acid-catalyzed heterolytic cleavage of the benzyl alcohols coupled with dehydration converts these molecules to QMs **16–19** (Scheme 8). Although these QMs can be represented by quinoidal structural formulas (compared to **15**), quantum yield of their formation is probably lower than for the corresponding *meta* derivative, as suggested from the quantum efficiency for the photomethanolysis reaction (the *meta* effect). The acid catalyzed photosolvolysis reaction at pH 2.4 suggests that, in acidic media, formation of QMs and photomethanolysis may take place also *via* the cationic species **16H⁺–19H⁺**. However, at neutral pH this represents only a minor pathway, since photomethanolysis of the methoxy derivatives **7'–10'** takes place with significantly lower quantum yields than for the free phenolic species. QMs **16–19** were detected by LFP in $\text{CH}_3\text{CN}-\text{H}_2\text{O}$ and in TFE. These are relatively stable species reacting slowly and selectively with nucleophiles (*e.g.* lifetime of **17** in aqueous CH_3CN is 1.2 ms). Inefficient incorporation of deuterium on photolysis in $\text{CH}_3\text{CN}-\text{D}_2\text{O}$ suggests that only one type of QMs are formed, that is, formal solvent-assisted proton transfer from the phenol



to the carbon atoms giving QM **23** probably does not take place.

Antiproliferative study

To investigate if the photochemically generated QMs could lead to antiproliferative activity, compounds **1** and **7-9** were subjected to preliminary antiproliferative testing on a colon carcinoma cell line HCT 116 (Table 4 and Fig. 5). The series of compounds was chosen to probe if the structure of the biphenyl QM could be correlated to the activity. Trioxsalen (2,5,9-trimethyl-7H-furo[3,2-g]chromen-7-one) was used as a positive reference compound that is known to

exhibit antiproliferative activity on photoactivation.^{6a} The results demonstrated that without the irradiation the compounds exert antiproliferative activity towards this cell line ($IC_{50} \approx 18-68 \mu M$), predominantly at the maximal tested concentration (100 μM). Interestingly, the least active compound **7**, which did not cause the 50% growth inhibition even at the maximal tested concentration, was the only compound that exhibited a significant activity enhancement upon irradiation at 300 nm (3×1 min), resulting in an IC_{50} in the low micromolar range (9 μM) (Fig. 5). This result cannot be compared to the reference compound trioxsalen, which was significantly more potent after the irradiation. However, it is comparable to some of the binol-amino acid conjugates

Table 4 IC₅₀ values (in μM)^a

Compound	HCT 116 cell line
1	19 ± 1
7	>100
7^c	9 ± 1
8	18 ± 1
9	68 ± 7
trioxsalen	>100
trioxsalen ^b	1 ± 0.2
trioxsalen ^c	0.3 ± 0.2

^a IC₅₀; the concentration that causes 50% growth inhibition. ^b Irradiated 1 min at 300 nm with 6 lamps. ^c Irradiated 3 × 1 min at 300 nm with 6 lamps.

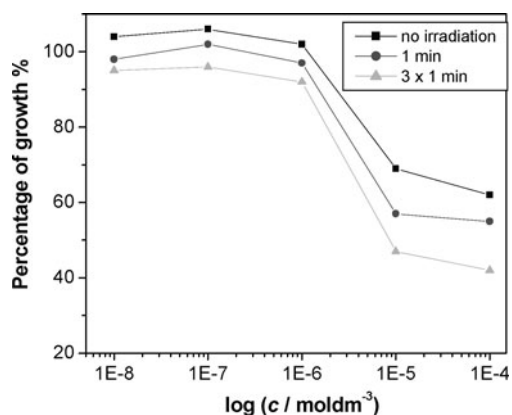


Fig. 5 Concentration-response profiles for compound **7** tested on HCT 116 cell line, without irradiation, or after the irradiation at 300 nm (1 min, or 3 × 1 min).

(p-BQMPs) described by Freccero *et al.* that are similarly not cytotoxic towards another colon carcinoma cell line (HT29), but upon irradiation the IC₅₀ concentrations reach 9–30 μM values.^{6a} Since **8** did not show increased activity on irradiation, the preliminary result suggests that the activity cannot be correlated only to the lifetimes of the generated QMs and their reactivity with nucleophiles. Probably, the structure of the QM, as well as the interplay between the lipophilicity (and membrane permeability) and solubility of the phenols in H₂O play an important role that is, however, yet to be investigated.

Conclusion

We have synthesized 4-phenylphenol derivatives **5–9** substituted with the sterically congested adamantyl moiety or two phenyl groups. In aqueous media in the singlet excited state, **5–9** undergo solvent assisted deprotonation of the phenol and protonation of the benzyl alcohol moiety, giving rise to QMs. The QMs react with nucleophilic solvent (except the *ortho* derivative **14**, which cyclizes to fluorene) giving rise to photosolvolytic products with high quantum yields ($\Phi \sim 0.1–0.5$). The zwitterionic QM **15** formed from **6** in TFE was characterized by LFP ($\tau \sim 250$ ns). The *para* QM derivatives **16–19** were detected by LFP in CH₃CN–H₂O and TFE solutions. In TFE, the adamantyl QM derivative **16** has a lifetime of 500 μs, whereas QM **17**, which has additional stabilization by two phenyl rings, has a particularly long lifetime of 1.1 s. The long lifetimes and selectivity in the reaction with N-nucleophiles renders this class of sterically congested transient

species potentially useful in biological systems for the alkylation of DNA. Preliminary investigation of the antiproliferative activity of photogenerated QMs was investigated for phenols **1**, and **7–9** on the HCT 116 human cancer cell line. It was shown that **7** on irradiation exhibits a 10 × increase in the antiproliferative activity.

Experimental

General

¹H and ¹³C NMR spectra were recorded on a Bruker AV-300, 500 or 600 MHz. The NMR spectra were taken in CDCl₃ or DMSO-d₆ at rt using TMS as a reference and chemical shifts were reported in ppm. Melting points were determined using an original Köfeler Mikroheitzsch apparatus (Reichter, Wien) and were not corrected. UV-vis spectra were recorded on a Varian Cary 100 Bio spectrophotometer at rt. IR spectra were recorded on a FT-IR-ABB Bomem MB 102 spectrophotometer in KBr. MS were recorded on an Agilent 6410 Triple Quadrupole Mass Spectrometer by use of the electrospray ionization technique. The spectra were obtained in the positive and negative mode in the presence of formic acid. HRMS were obtained on an Applied Biosystems 4800 Plus MALDI TOF/TOF instrument (AB, Foster City, CA). For the sample analysis a Shimadzu HPLC equipped with a Diode-Array detector and a Phenomenex Luna 3u C18(2) column was used. Mobile phase was CH₃OH–H₂O (20%). For the chromatographic separations silica gel (Merck 0.05–0.2mm) was used. Analytical thin layer chromatography was performed on Polygram® SILG/UV₂₅₄ (Machery-Nagel) plates. Irradiation experiments were performed in a Rayonet reactor equipped with 16 lamps with the output at 254 nm or a Luzchem reactor equipped with 8 lamps. During irradiations in the Rayonet, the irradiated solutions were continuously purged with Ar and cooled by a tap-water finger-condenser. Solvents for irradiation were of HPLC purity. Chemicals (dibromobenzenes, bromoanisoles, 2-adamantanone, solution of BBr₃) were purchased from the usual commercial sources and were used as received. Solvents for chromatographic separations were purified by distillation.

General procedure for the Grignard reaction

The reaction was carried out in a two-neck round bottom flask (100 mL) under a N₂ inert atmosphere equipped with a condenser and a dropping funnel. Magnesium (10 mmol), which was freshly activated prior to reaction, was placed in the flask and suspended in THF (10 mL). In the dropping funnel was placed THF solution (20 mL) of bromobiphenyl (10 mmol). A few drops of the solution were added to the suspension in the flask and the reaction was initiated by adding a crystal of iodine and heating. The remaining solution in the funnel was added over 30 min at rt. After the addition was completed, the reaction mixture was refluxed until all the magnesium reacted (1–1.5 h). The solution of the Grignard reagent was cooled to rt and a THF solution (20 mL) of ketone (10 mmol) was added dropwise during 1 h. After addition was completed, the reaction mixture was refluxed for 4 h and stirred at rt over night. The next day, saturated solution of ammonium chloride (100 mL) was added to the reaction mixture, the layers were separated, and the aqueous layer additionally acidified with 1 M HCl until all solid dissolved. The acidified aqueous layer was

extracted with diethyl ether (3 × 30 mL), organic extracts combined and dried over anhydrous MgSO₄. After filtration and removal of the solvent, the crude product was obtained that was additionally purified by chromatography on silica gel using CH₂Cl₂ or CH₂Cl₂–EtOAc as an eluent.

2-(2-hydroxyadamantan-2-yl)-4'-methoxybiphenyl (5')

The Grignard reagent was prepared from 2-bromo-4'-methoxybiphenyl (1.65 g, 6.3 mmol) and magnesium (0.17 g, 7.0 mmol), and reacted with 2-adamantanone (1.02 g, 6.8 mmol) to afford 2.6 g of the crude product that was purified on a column of silica gel to give the product (1.69 g, 79%) in the form of colorless crystals that were crystallized from CCl₄/hexane.

mp 125–130 °C; IR (KBr) ν /cm⁻¹: 3448, 3396, 2897; ¹H NMR (CDCl₃, 600 MHz) δ (ppm): 7.61 (d, 1H, *J* = 8.0 Hz), 7.32 (t, 1H, *J* = 8.0 Hz), 7.28 (d, 2H, *J* = 8.5 Hz), 7.25 (t, 1H, *J* = 8.0 Hz), 7.10 (d, 2H, *J* = 8.5 Hz), 3.84 (s, 3H), 2.27 (s, 2H), 2.17 (br s, 1H), 2.15 (br s, 1H), 1.81 (s, 1H), 1.73 (br s, 1H), 1.62–1.69 (m, 3H), 1.60 (br s, 2H), 1.52–1.57 (m, 2H), 1.49 (d, 2H, *J* = 12.4 Hz); ¹³C NMR (CDCl₃, 75 MHz) δ (ppm): 158.31 (s), 141.99 (s, 2C), 137.16 (s), 133.77 (d), 129.90 (d, 2C), 126.88 (d), 126.82 (d), 126.40 (d), 112.99 (d, 2C), 77.77 (s), 55.12 (q), 37.50 (t), 34.94 (d, 2C), 34.71 (t, 2C), 32.92 (t, 2C), 27.20 (d), 26.33 (d); HRMS (MALDI) calculated for C₂₃H₂₆O₂ (+H⁺–H₂O) 317.1900, found 317.1891.

3-(2-hydroxyadamantan-2-yl)-4'-methoxybiphenyl (6')

The Grignard reagent was prepared from 3-bromo-4'-methoxybiphenyl (1.67 g, 6.4 mmol) and magnesium (0.17 g, 7.0 mmol), and reacted with 2-adamantanone (1.05 g, 7.0 mmol) to afford 2.3 g of the crude product that was purified on a column of silica gel to give the product (1.66 g, 78%) in the form of colorless crystals.

mp 103–105 °C; IR (KBr) ν /cm⁻¹: 3517, 3049, 2909, 2846; ¹H NMR (CDCl₃, 300 MHz) δ (ppm): 7.71 (br s, 1H), 7.51 (d, 2H, *J* = 8.8 Hz), 7.27–7.49 (m, 3H), 6.97 (d, 2H, *J* = 8.8 Hz), 3.84 (s, 3H), 2.62 (br s, 2H), 2.45 (br s, 1H), 2.41 (br s, 1H), 1.91 (br s, 1H), 1.68–1.80 (m, 10H); ¹³C NMR (CDCl₃, 75 MHz) δ (ppm): 159.07 (s), 145.74 (s), 141.16 (s), 133.93 (s), 128.96 (d), 128.12 (d, 2C), 125.65 (d), 123.94 (d), 123.69 (d), 114.10 (d, 2C), 75.63 (s), 55.24 (q), 37.60 (t), 35.67 (d, 2C), 34.87 (t, 2C), 32.90 (t, 2C), 27.36 (d), 26.86 (d). HRMS (MALDI) calculated for C₂₃H₂₆O₂ (+H⁺–H₂O) 317.1900, found 317.1894.

4-(2-hydroxyadamantan-2-yl)-4'-methoxybiphenyl (7')

The Grignard reagent was prepared from 4-bromo-4'-methoxybiphenyl (1.71 g, 6.5 mmol) and magnesium (0.18 g, 7.5 mmol), and reacted with 2-adamantanone (1.14 g, 7.6 mmol) to afford 2.38 g of the crude product that was purified on a column of silica gel to give the product (1.62 g, 65%) in the form of colorless crystals.

mp 186–187 °C; IR (KBr) ν /cm⁻¹: 3563, 2928, 2897, 2854; ¹H NMR (CDCl₃, 300 MHz) δ (ppm): 7.58 (d, 2H, *J* = 8.8 Hz), 7.54 (d, 2H, *J* = 8.8 Hz), 7.53 (d, 2H, *J* = 8.8 Hz), 6.97 (d, 2H, *J* = 8.8 Hz), 3.84 (s, 3H), 2.59 (br s, 2H), 2.45 (br s, 1H), 2.40 (br s, 1H), 1.91 (br s, 1H), 1.70–1.80 (m, 10H); ¹³C NMR (CDCl₃, 75 MHz) δ (ppm): 159.07 (s), 143.67 (s), 139.54 (s), 133.12 (s), 127.90 (d), 126.79 (d), 125.74 (d), 114.11 (d), 75.41 (s), 55.20 (q), 37.60

(t), 35.61 (d, 2C), 34.84 (t, 2C), 32.88 (t, 2C), 27.36 (d), 26.86 (d); HRMS (MALDI) calculated for C₂₃H₂₆O₂ (+H⁺–H₂O) 317.1900, found 317.1912.

(4'-methoxybiphenyl-4-yl)diphenylmethanol (8')³⁴

The Grignard reagent was prepared from 4-bromo-4'-methoxybiphenyl (1.16 g, 4.41 mmol) and magnesium (0.12 g, 4.8 mmol), and reacted with benzophenone (0.80 g, 4.41 mmol) to afford 1.57 g of the crude product that was purified on a column of silica gel to give the product (0.82 g, 51%) in the form of colorless crystals.

Colorless crystals, mp 86–87 °C; ¹H NMR (CDCl₃, 600 MHz) δ (ppm): 7.51 (d, 2H, *J* = 8.8 Hz), 7.48 (d, 2H, *J* = 8.5 Hz), 7.30–7.34 (m, 10H), 7.28 (dd, 2H, *J* = 8.1 Hz, *J* = 8.5 Hz), 6.95 (d, 2H, *J* = 8.8 Hz), 3.83 (s, 3H), 2.81 (br s, 1H OH); ¹³C NMR (CDCl₃, 125 MHz) δ (ppm): 159.11 (s), 146.78 (s), 145.17 (s), 139.54 (s), 133.06 (s), 128.23 (d, 2C), 127.96 (d, 2C), 127.85 (d, 4C), 127.82 (d, 4C), 127.17 (d, 2C), 126.05 (d, 2C), 114.13 (d, 2C), 81.80 (s), 55.21 (q); HRMS (MALDI) calculated for C₂₆H₂₂O₂ (–e⁻) 366.1625, found 366.162.

4-(2-hydroxypropan-2-yl)-4'-methoxybiphenyl (9')³⁵

The Grignard reagent was prepared from 4-bromo-4'-methoxybiphenyl (1.0 g, 3.81 mmol) and magnesium (0.10 g, 4.2 mmol), and reacted with acetone (5 mL) to afford 1.05 g of the crude product that was purified on a column of silica gel to give the product (0.50 g, 54%) in the form of colorless crystals.

Colorless crystals, mp 122–124 °C; ¹H NMR (CDCl₃, 300 MHz) δ (ppm): 7.48–7.54 (m, 6H), 6.96 (d, 2H, *J* = 8.8 Hz), 3.83 (s, 3H), 1.81 (brs, 1H, OH), 1.61 (s, 6H); ¹³C NMR (CDCl₃, 75 MHz) δ (ppm): 159.01 (s), 147.43 (s), 139.12 (s), 133.29 (s), 127.93 (d), 126.40 (d), 124.72 (d), 114.11 (d), 72.29 (s), 55.21 (q), 31.64 (q); HRMS (MALDI) calculated for C₁₆H₁₈O₂ (–e⁻) 242.1312, found 242.1314.

General procedure for the removal of the methoxy groups from phenols with BBr₃

The reaction was carried out under N₂-atmosphere in a three-neck round bottom flask (250 mL) equipped with a septum and a syringe. In the flask was placed methoxybiphenyl derivative (10 mmol), dissolved in dry CH₂Cl₂ (100 mL) and the solution cooled to 0 °C by ice-bath. To the cold solution, a solution of BBr₃ in CH₂Cl₂ (1 M, 30 mL) was added dropwise over 1 h using a syringe. After the addition was completed, the stirring was continued for 1 h at 0 °C, and at rt over night. The next day 100 mL of cold water was added to the reaction mixture, the layers were separated and the aqueous layer extracted with CH₂Cl₂ (3 × 50 mL). The combined organic extracts were dried over anhydrous MgSO₄, solid was removed by filtration and solvent removed on a rotary evaporator. The obtained crude product was purified on a column filled with silica gel by use of CH₂Cl₂ and CH₂Cl₂–EtOAc (4 : 1) as eluent, and crystallization.

3-(2-hydroxyadamantan-2-yl)-4'-hydroxybiphenyl (6)

From 3-(2-hydroxyadamantan-2-yl)-4'-methoxybiphenyl (6', 1.23 g, 3.7 mmol) and solution of BBr₃ (1 M, 12 mL), the reaction gave

1.55 g of the crude product that was purified by crystallization from mixture of ethyl acetate and hexane to afford 0.94 g (79%) of the pure product in a form of colorless crystals.

mp 155–157 °C; IR (KBr) ν/cm^{-1} : 3499, 3462, 3360, 2908, 2853; ^1H NMR (DMSO- d_6 , 300 MHz) δ (ppm): 9.50 (br s, OH), 7.63 (br s, 1H), 7.46 (d, 2H, $J = 8.6$ Hz), 7.35–7.44 (m, 3H), 6.85 (d, 2H, $J = 8.0$ Hz), 2.52 (br s, 2H), 2.42 (br s, 1H), 2.38 (br s, 1H), 1.81 (br s, 1H), 1.55–1.70 (m, 10H); ^{13}C NMR (DMSO- d_6 , 75 MHz) δ (ppm): 156.45 (s), 146.10 (s), 139.52 (s), 131.07 (s), 128.07 (d), 127.22 (d, 2C), 123.61 (d), 123.33 (d), 122.93 (d), 115.19 (d, 2C), 73.09 (s), 36.93 (t), 34.29 (d, 2C), 33.85 (t, 2C), 32.08 (t, 2C), 26.46 (d), 26.07 (d); HRMS (MALDI) calculated for $\text{C}_{22}\text{H}_{24}\text{O}_2$ ($+\text{H}^+ - \text{H}_2\text{O}$) 303.1743, found 303.1754.

4-(2-hydroxyadamantan-2-yl)-4'-hydroxybiphenyl (7)

From 4-(2-hydroxyadamantan-2-yl)-4'-methoxybiphenyl (**7'**, 1.40 g, 4.2 mmol) and solution of BBr_3 (1 M, 13 mL), the reaction gave 1.35 g of the crude product that was purified by crystallization from ethyl acetate to afford 0.9 g (67%) of the pure product in a form of colorless crystals.

mp 225–228 °C; IR (KBr) ν/cm^{-1} : 3431, 3190, 2924, 2856; ^1H NMR (DMSO- d_6 , 300 MHz) δ (ppm): 9.48 (br s, OH), 7.42–7.61 (m, 6H), 6.84 (d, 2H, $J = 8.5$ Hz), 2.47 (br s, 2H), 2.41 (br s, 1H), 2.38 (br s, 1H), 1.81 (br s, 1H), 1.53–1.73 (m, 10H); ^{13}C NMR (DMSO- d_6 , 75 MHz) δ (ppm): 156.94 (s), 144.26 (s), 138.14 (s), 130.77 (s), 127.49 (d, 2C), 126.05 (d, 2C), 125.59 (d, 2C), 115.67 (d, 2C), 73.34 (s), 37.44 (t), 34.80 (d, 2C), 34.34 (s, 2C), 32.55 (s, 2C), 26.97 (d), 26.57 (d); HRMS (MALDI) calculated for $\text{C}_{22}\text{H}_{24}\text{O}_2$ ($+\text{H}^+ - \text{H}_2\text{O}$) 303.1743, found 303.1740.

Spiro[adamantane-2,9'-(2'-hydroxy)fluorene] (11)

From 2-(2-hydroxyadamantan-2-yl)-4'-methoxybiphenyl (**5'**, 0.18 g, 0.54 mmol) and solution of BBr_3 (1 M, 4 mL), the reaction gave 0.17 g of the crude product that was purified by crystallization from mixture of ethyl acetate and hexane to afford 100 mg (59%) of the pure product in a form of colorless crystals.

mp 254–256 °C; IR (KBr) ν/cm^{-1} : 3302, 2973, 2888; ^1H NMR (CDCl_3 , 300 MHz) δ (ppm): 8.06 (d, 1H, $J = 8.0$ Hz), 7.67 (dd, 1H, $J = 7.5$ Hz, $J = 0.9$ Hz), 7.60–7.65 (m, 2H), 7.33 (dt, 1H, $J = 7.5$ Hz, $J = 0.8$ Hz), 7.21 (dt, 1H, $J = 7.9$ Hz, $J = 1.3$ Hz), 6.85 (dd, 1H, $J = 8.1$ Hz, $J = 2.3$ Hz), 4.76 (br s, 1H, OH), 2.83–2.97 (m, 4H), 2.15–2.22 (m, 2H), 1.98 (br s, 2H), 1.73–1.83 (m, 4H), 1.55–1.64 (m, 2H); ^{13}C NMR (CDCl_3 , 125 MHz) δ (ppm): 153.79 (s), 152.82 (s), 150.33 (s), 140.62 (s), 133.94 (s), 129.16 (d), 126.78 (d), 124.71 (d), 119.80 (d), 118.48 (d), 117.14 (d), 113.84 (d), 58.42 (s), 41.38 (t), 34.75 (d, 2C), 34.15 (t, 2C), 33.95 (t, 2C), 27.26 (d), 27.18 (d); HRMS (MALDI) calculated for $\text{C}_{22}\text{H}_{20}\text{O}$ ($+\text{H}^+$) 303.1743, found 303.1735.

4'-(hydroxydiphenylmethyl)biphenyl-4-ol (8)³⁴

From 4'-methoxybiphenyl-4-yl)diphenylmethanol (**8'**, 0.82 g, 2.4 mmol) and solution of BBr_3 (1 M, 10 mL), the reaction gave 0.67 g of the crude product that was purified by crystallization from a mixture of carbon tetrachloride, toluene and ether to afford 0.57 g (83%) of the pure product in a form of colorless crystals.

mp 274–276 °C; ^1H NMR (CDCl_3 , 300 MHz) δ (ppm): 9.50 (br s, 1H, OH), 7.49 (t, 4H, $J = 8.7$ Hz), 7.18–7.34 (m, 12H), 6.83

(d, 2H, $J = 8.6$ Hz), 6.41 (br s, 1H, OH); ^{13}C NMR (CDCl_3 , 125 MHz) δ (ppm): 157.05 (s), 147.75 (s, 2C), 145.84 (s), 138.47 (s), 130.52 (s), 128.23 (d, 2C), 127.72 (d, 4C), 127.62 (d, 2C), 127.50 (d, 4C), 126.59 (d, 2C), 125.03 (d, 2C), 115.66 (d, 2C), 80.38 (s); HRMS (MALDI) calculated for $\text{C}_{25}\text{H}_{20}\text{O}_2$ ($-e^-$) 352.1469, found 352.1461.

General procedure for the removal of the methoxy groups from phenols with thiolate

The reaction was carried out under a N_2 -atmosphere in a round-bottom flask (100 mL) equipped with a condenser and a dropping funnel, and the outlet of the N_2 from the condenser was purged through a solution of sodium ethoxide in ethanol. In the flask was placed sodium hydride (0.46 g, 20 mmol) and suspended in 5 mL of dry DMF. The suspension was cooled by ice-bath and a solution of ethyl mercaptane (1.4 mL, 20 mmol) in DMF (5 mL) was added dropwise. When the addition was completed, the reaction mixture was stirred for 10 min and the ice-bath was removed. Methoxybiphenyl derivative (1.7 g, 5.08 mmol) was dissolved in DMF (10 mL) and added to the reaction mixture. After addition, the mixture was refluxed over 4 h, cooled, and poured into 100 mL of H_2O . The aqueous mixture was washed with hexane (2×50 mL) and acidified by saturated solution of ammonium chloride. Extraction with ethyl acetate was carried out (3×100 mL), extracts dried over anhydrous MgSO_4 , solid removed by filtration, and solvent removed on the rotary evaporator. The reaction furnished the crude product that was purified by chromatography and crystallization.

2-(2-hydroxyadamantan-2-yl)-4'-hydroxybiphenyl (5)

From 2-(2-hydroxyadamantan-2-yl)-4'-methoxybiphenyl (**5'**, 0.90 g, 2.67 mmol), sodium hydride (0.5 g, 21 mmol) and ethyl mercaptane (780 μL , 11 mmol) in DMF (10 mL) the reaction gave 900 mg of the crude product that was purified by crystallization from mixture of ethyl acetate and hexane to afford 600 mg (69%) of the pure product in a form of colorless crystals.

mp 160–163 °C; ^1H NMR (DMSO- d_6 , 300 MHz) δ (ppm): 9.29 (s, 1H, OH), 7.55 (d, 1H, $J = 7.7$ Hz), 7.29 (t, 1H, $J = 7.7$ Hz), 7.16–7.26 (m, 3H), 6.98 (dd, 1H, $J = 1.0$ Hz, $J = 7.2$ Hz), 6.70 (d, 2H, $J = 8.4$ Hz), 4.73 (s, 1H, OH), 2.10–2.30 (m, 4H), 1.20–1.70 (m, 10H); ^{13}C NMR (DMSO- d_6 , 75 MHz) δ (ppm): 158.82 (s), 142.53 (s), 142.26 (s), 135.54 (s), 133.40 (d), 130.12 (d, 2C), 127.11 (d), 126.27 (d), 126.00 (d), 114.16 (d, 2C), 75.70 (s), 37.34 (t), 34.28 (t, 2C), 34.08 (d, 2C), 32.62 (t, 2C), 26.78 (d), 26.13 (d); HRMS (MLADI) calculated for $\text{C}_{22}\text{H}_{24}\text{O}_2$ ($+\text{H}^+ - \text{H}_2\text{O}$) 303.1743, found 303.1754.

4-hydroxy-4'-(2-hydroxypropan-2-yl)biphenyl (9)³⁶

From 4-methoxy-4'-(2-hydroxypropan-2-yl)biphenyl (**9'**, 0.40 g, 1.65 mmol), sodium hydride (0.3 g, 6.61 mmol) and ethyl mercaptane (480 μL , 6.61 mmol) in DMF (10 mL) the reaction gave a crude product that was purified by chromatography on silica gel using dichloromethane–ethyl acetate (7 : 3) to afford 0.30 g (80%) of the pure product in the form of colorless crystals.

mp 178–180 °C; ^1H NMR (DMSO- d_6 , 300 MHz), δ (ppm): 9.48 (s, 1H, OH), 7.48 (s, 4H), 7.45 (d, 2H, $J = 8.6$ Hz), 6.83 (d, 2H, $J = 8.6$ Hz), 4.98 (br s, 1H, OH), 1.44 (s, 6H); ^{13}C NMR

(DMSO-*d*₆, 75 MHz) δ (ppm): 156.87 (s), 148.60 (s), 137.86 (s), 130.94 (s), 127.52 (d, 2C), 125.31 (d, 2C), 124.98 (d, 2C), 115.64 (d, 2C), 70.47 (s), 31.90 (q, 2C); HRMS (MALDI) calculated for C₁₅H₁₆O₂ (-e⁻) 228.1156, found 228.1156.

Photochemical experiments, general

In a quartz vessel was placed a CH₃OH, or CH₃OH–H₂O (3 : 1 or 4 : 1), solution (100 mL, *c* ~ 10⁻³ M) of biphenyl **5–8** (20–100 mg) and irradiated in a Rayonet reactor using 16 lamps at 254 nm for 1 min–1 h. Prior to and during the irradiation, the solution was continuously purged with a stream of Ar and cooled by a cold-finger condenser. After irradiation, CH₃OH was removed on a rotary evaporator and the residue (if irradiated in CH₃OH–H₂O) extracted with EtOAc (3 × 75 mL). Extracts were dried over anhydrous MgSO₄, filtered and solvent was removed on a rotary evaporator. The residue was chromatographed on a thin layer of silica gel using CH₂Cl₂–EtOAc (30%) as eluents.

Irradiation of 5. (80 mg, 0.16 mmol) in 100 mL CH₃OH for 2 h gave, after evaporation of the solvent and chromatographic separation using CH₂Cl₂–EtOAc (30%) as eluents, 10 mg (12%) of product **11**, 30 mg (38%) of product **6** and 30 mg of the starting material.

Irradiation of 6. (20 mg, 0.31 mmol) in 100 mL CH₃OH–H₂O (3 : 1) for 15 min gave, after evaporation of the solvent and chromatographic separation using CH₂Cl₂–EtOAc (30%) as eluents, 20 mg (95%) of product **6OMe**.

3-(2-methoxyadamantan-2-yl)-4'-hydroxybiphenyl (6OMe). Colorless crystals, mp 174–178 °C; ¹H NMR (CDCl₃, 300 MHz) δ (ppm): 7.66 (br s, 1H), 7.35–7.50 (m, 5H), 6.89 (d, 2H, *J* = 8.6 Hz), 5.65 (br s, 1H, OH), 2.88 (s, 3H, OCH₃), 2.71 (br s, 2H), 2.37 (br s, 1H), 2.33 (br s, 1H), 1.91 (br s, 1H), 1.60–1.80 (m, 9H); ¹³C NMR (CDCl₃, 75 MHz) δ (ppm): 155.28 (s), 141.18 (s), 140.55 (s), 133.84 (s), 128.30 (d, 2C), 128.14 (d), 125.72 (d), 125.59 (d), 125.46 (d), 115.56 (d, 2C), 80.36 (s), 40.03 (q), 37.56 (t), 34.46 (t, 2C), 32.74 (t, 2C), 27.59 (d), 26.73 (d); HRMS (MALDI) calculated for C₂₃H₂₆O₂ (+H⁺-OCH₃) 303.1743, found 303.1757.

Irradiation of 7. (70 mg, 0.31 mmol) in 500 mL CH₃OH–H₂O (4 : 1) for 1 h gave mixture of **7** and **7OMe**. After evaporation of the CH₃OH, the aqueous residue was extracted with EtOAc (3 × 75 mL). The extracts were dried, filtered and solvent was removed. The residue was analyzed by HPLC. It contained **7** and **7OMe** in a ratio 1 : 3.

The pure product **7OMe** was obtained by stirring **7** (50 mg) in CH₃OH (50 mL) in the presence of H₂SO₄ (500 mg) overnight. The next day, to the solution NaHCO₃ (860 mg) was added and stirring was continued over 4 h. The mixture was filtered and solvent evaporated to afford **7OMe** for the analysis by NMR.

4-(2-methoxyadamantan-2-yl)-4'-hydroxybiphenyl (7OMe). Colorless crystals, mp 180–181 °C; ¹H NMR (DMSO-*d*₆, 300 MHz) δ (ppm): 9.48 (br s, 1H, OH), 7.57 (d, 2H, *J* = 8.5 Hz), 7.49 (d, 2H, *J* = 8.6 Hz), 7.46 (d, 2H, *J* = 8.5 Hz), 6.84 (d, 2H, *J* = 8.6 Hz), 2.71 (s, 3H, OCH₃), 2.61 (br s, 2H), 2.23 (br s, 1H), 2.19 (br s, 1H), 1.82 (br s, 1H), 1.50–1.72 (m, 9H); ¹³C NMR (DMSO-*d*₆, 75 MHz) δ (ppm): 157.20 (s), 138.83 (s), 138.65 (s), 130.49 (s), 127.72 (d, 2C), 127.68 (d, 2C), 125.52

(d, 2C), 115.82 (d, 2C), 79.08 (s), 47.65 (q), 37.25 (t), 34.18 (t, 2C), 32.45 (t, 2C), 32.11 (d, 2C), 27.18 (d), 26.35 (d); HRMS (MALDI) calculated for C₂₃H₂₆O₂ (+H⁺-OCH₃) 303.1743, found 303.1742.

Irradiation of 8. (100 mg, 0.28 mmol) in 100 mL CH₃OH for 30 min gave, after evaporation of the solvent and chromatographic separation using CH₂Cl₂–EtOAc (30%) as eluents, 10 mg (10%) of product **8OMe** and 90 mg of the starting material.

4'-(methoxydiphenylmethyl)biphenyl-4-ol (8OMe). Colorless crystals, mp 178–182 °C; ¹H NMR (CDCl₃, 500 MHz) δ (ppm): 7.43–7.48 (m, 8H), 7.26–7.32 (m, 4H), 7.20–7.25 (m, 2H), 7.14 (d, 2H, *J* = 8.1 Hz), 6.86 (d, 2H, *J* = 8.7 Hz), 5.04 (br s, 1H, OH), 3.08 (s, 3H, OCH₃); ¹³C NMR (CDCl₃, 125 MHz) δ (ppm): 155.02 (s), 143.84 (s), 142.25 (s), 139.05 (s), 133.27 (s), 129.02 (d, 2C), 128.61 (d, 4C), 128.14 (d, 2C), 127.69 (d, 4C), 126.83 (d, 2C), 125.86 (d, 2C), 115.52 (d, 2C), 52.00 (q); HRMS (MALDI) calculated for C₂₆H₂₂O₂ (+H⁺-OCH₃) 335.1441, found 335.1455.

Irradiation of 9. (60 mg mmol) in 100 mL CH₃OH for 1 h gave, after evaporation of the solvent and chromatographic separation using CH₂Cl₂–EtOAc (2%), 10 mg of product **12**, and 10 mg of product **9OMe**, as well as 40 mg of the starting material.

4-hydroxy-4'-(prop-1-en-2-yl)biphenyl (12)³⁷. Colorless crystals, ¹H NMR (CDCl₃, 500 MHz) δ (ppm): 7.48–7.52 (m, 4 H), 7.47 (d, 2H, *J* = 8.7 Hz), 6.88 (d, 2H, *J* = 8.7 Hz), 5.39–5.40 (m, 1H), 5.08 (q, 1H, *J* = 1.5 Hz), 4.85 (br s, 1H, OH), 2.16 (dd, 3H, *J* = 0.7 Hz, *J* = 1.5 Hz); ¹³C NMR (CDCl₃, 125 MHz) δ (ppm): 155.02 (s), 142.69 (s), 139.64 (s), 139.46 (s), 133.46 (s), 128.11 (d, 2C), 126.34 (d, 2C), 125.76 (d, 2C), 115.56 (d, 2C), 112.11 (t), 23.91 (q); RMS (MALDI) calculated for C₁₅H₁₄O (-e⁻) 210.1050, found 210.1047.

4-hydroxy-4'-(2-methoxypropan-2-yl)biphenyl (9OMe). Colorless crystals, mp 126–132 °C; IR (KBr) ν_{max} /cm⁻¹: ¹H NMR (CDCl₃, 500 MHz) δ (ppm): 7.50 (d, 2H, *J* = 8.6 Hz), 7.47 (d, 2H, *J* = 8.6 Hz), 7.43 (d, 2H, *J* = 8.6 Hz), 6.89 (d, 2H, *J* = 8.6 Hz), 5.14 (br s, 1H, OH), 3.09 (s, 3H, OCH₃), 1.55 (s, 6H, CH₃); ¹³C NMR (CDCl₃, 125 MHz) δ (ppm): 155.04 (s), 144.13 (s), 139.18 (s), 133.42 (s), 128.16 (d, 2C), 126.35 (d, 2C), 126.15 (d, 2C), 115.54 (d, 2C), 50.58 (q), 27.84 (q, 2C), one singlet is covered by CDCl₃; HRMS (MALDI) calculated for C₁₅H₁₄O (+Na⁺) 265.1199, found 265.1205.

Quantum yields for the photomethanolysis reaction

Solutions of **5–8** and a solution of 2-hydroxybenzyl alcohol in CH₃CN–H₂O (1 : 1), as well as a solution of valerophenone in CH₃CN–H₂O (1 : 1) were freshly prepared and their concentrations adjusted to have absorbances at 254 nm 0.4–0.8. After adjustment of the concentration and measurement of the corresponding UV-vis spectra the solutions were put in quartz cuvettes (20 mL), purged with a stream of N₂ (20 min each), and sealed with a septum. The cuvettes were irradiated at the same time in a Luzchem reactor equipped with a carousel and 8 lamps with the output at 254 nm for 0.5, 1, and 4 min. After each irradiation, the samples were taken from the cuvettes by use of a syringe and analyzed by HPLC. Quantum yields for the methanolysis were calculated using the quantum yield for the methanolysis of 2-hydroxybiphenyl (Φ = 0.23)¹² and the Norrish-II cleavage

(formation of acetophenone) of valerophenone in aqueous media ($\Phi = 0.65 \pm 0.03$).²¹

Irradiation in CH₃CN–D₂O

To a solution of **6**, **7**, or **11** (10 mg, 0.018 mmol) in CH₃CN (90 mL) was added 10 mL of D₂O. The solution was purged with Ar for 30 min and irradiated in a Rayonet reactor at 254 nm (16 lamps) for 1 h. During irradiation, the solution was continuously purged with Ar and cooled by a cold-finger condenser. After irradiation, 50 mL of H₂O was added and extractions with EtOAc (3 × 75 mL) were carried out. The extracts were dried over anhydrous MgSO₄. After filtration and evaporation of the solvent, the crude mixture was analyzed by NMR and MS.

Steady state and time-resolved fluorescence measurements

The steady state measurements were performed on a Photon Technology International (PTI) Quanta-Master QM-2 luminescence spectrometer. The samples were dissolved in CH₃CN, or CH₃CN–H₂O (4 : 1) and the concentrations were adjusted to have absorbances at the excitation wavelength (270 nm) < 0.1. Solutions were purged with nitrogen for 30 min prior to analysis. The measurements were performed at 20 °C. Fluorescence quantum yields were determined by comparison of the integral of the emission bands with the one of fluorene in methanol ($\Phi = 0.68$).²⁵ Typically, three absorption traces were recorded (and averaged) and three fluorescence emission traces, exciting at three different wavelengths. Three quantum yields were calculated and the mean value reported.

Fluorescence titrations were performed by adding aliquots (60 μ L) of aqueous HClO₄ (pH = 2.10) to 2 mL of the CH₃CN–H₂O (4 : 1) solution. The pH of aqueous HClO₄ was measured by a pH meter. The titration was performed at 20 °C in air-saturated solutions.

Fluorescence decay histograms were obtained on an Edinburgh instrument OB920, equipped with a light emitting diode (excitation wavelength 265 nm), using time-correlated single photon counting technique in 1023 channels. Histograms of the instrument response functions (using LUDOX scatterer), and sample decays were recorded until they typically reached 3×10^3 counts in the peak channel (except for **5** where only 10^3 counts were collected). The half width of the instrument response function was typically ~1.5 ns. The time increment per channel was 0.049 or 0.098 ns. Obtained histograms were fitted as sums of an exponential using Gaussian-weighted non-linear least-squares fitting based on Marquardt–Levenberg minimization implemented in the software package of the instrument. The fitting parameters (decay times and pre-exponential factors) were determined by minimizing the reduced chi-square χ^2 . An additional graphical method was used to judge the quality of the fit that included plots of the weighted residuals vs. channel number.

Laser flash photolysis (LFP)

All LFP studies were conducted at the University of Victoria LFP facility employing a YAG laser, with a pulse width of 10 ns and excitation wavelength 266 nm. Static cells (0.7 cm) were used and solutions were purged with nitrogen or oxygen for 20 min prior to measurements. Absorbances at 266 nm were ~0.4–0.6.

Antiproliferative investigation

The experiments were carried out on a human colon carcinoma cell line HCT 116. Cells were cultured as monolayers and maintained in Dulbecco's modified Eagle medium (DMEM) supplemented with 10% fetal bovine serum (FBS), 2mM L-glutamine, 100 U mL⁻¹ penicillin and 100 μ g mL⁻¹ streptomycin in a humidified atmosphere with 5% CO₂ at 37 °C.

The cells were inoculated in parallel on three 96-well microtiter plates on day 0, at 1.5×10^4 cells mL⁻¹. Test agents were added in ten-fold dilutions (10^{-8} to 10^{-4} M) on the next day and incubated for a further 72 h. Working dilutions were freshly prepared on the day of testing. One of the plates was left in the dark, while the other was irradiated in a Luzchem reactor (6 lamps 300 nm, 1 min) four hours after the addition of the compounds. The third plate was additionally irradiated (6 lamps 300 nm, 1 min) 24 and 48 h after the first irradiation. After 72 h of incubation the cell growth rate was evaluated by performing the MTT assay^{38,39} which detects dehydrogenase activity in viable cells. The absorbance (*A*) was measured on a microplate reader at 570 nm. The absorbance is directly proportional to the number of living, metabolically active cells. The percentage of growth (PG) of the cell lines was calculated according to one or the other of the following two expressions:

If $(\text{mean } A_{\text{test}} - \text{mean } A_{\text{Izero}}) \geq 0$, then $\text{PG} = 100 \times (\text{mean } A_{\text{test}} - \text{mean } A_{\text{Izero}}) / (\text{mean } A_{\text{ctrl}} - \text{mean } A_{\text{Izero}})$.

If $(\text{mean } A_{\text{test}} - \text{mean } A_{\text{Izero}}) < 0$, then: $\text{PG} = 100 \times (\text{mean } A_{\text{test}} - \text{mean } A_{\text{Izero}}) / A_{\text{Izero}}$, where the mean A_{Izero} is the average of optical density measurements before exposure of cells to the test compound, the mean A_{test} is the average of optical density measurements after the desired period of time and the mean A_{ctrl} is the average of optical density measurements after the desired period of time with no exposure of cells to the test compound. In the experiments where the cells were irradiated, A_{ctrl} represents irradiated control cells, which typically showed 25% growth inhibition compared to A_{ctrl} without irradiation.

The results are expressed as IC₅₀, which is the concentration necessary for 50% of inhibition. The IC₅₀ values for each compound are calculated from concentration-response curves using linear regression analysis by fitting the test concentrations that give PG values above and below the reference value (*i.e.* 50%). If, however, all of the tested concentrations produce PGs exceeding the respective reference level of effect (*e.g.* PG value of 50), then the highest tested concentration is assigned as the default value, which is preceded by a ">" sign. Each test was performed in quadruplicate in at least two individual experiments.

Acknowledgements

These materials are based on work financed by the National Foundation for Science, Higher Education and Technological Development of the Republic of Croatia (HRZZ grant no. 02.05/25), the Ministry of Science Education and Sports of the Republic of Croatia (grant No. 098-0982933-2911), the Natural Sciences and Engineering Research Council (NSERC) of Canada and the University of Victoria.

Notes and references

- 1 *Quinone Methides*, ed. S. E. Rokita, Wiley, Hoboken, 2009.
- 2 E. Modica, R. Zanaletti, M. Freccero and M. Mella, Alkylation of amino acids and glutathione in water by *o*-quinone methide. Reactivity and selectivity, *J. Org. Chem.*, 2001, **66**, 41–52.

- 3 (a) Q. Zeng and S. E. Rokita, Tandem quinone methide generation for cross-linking DNA, *J. Org. Chem.*, 1996, **61**, 9080–9081; (b) S. E. Rokita, J. Yang, P. Pande and W. A. Greenberg, Quinone methide alkylation of deoxycytidine, *J. Org. Chem.*, 1997, **62**, 3010–3012.
- 4 (a) W. F. Velhuyzen, P. Pande and S. E. Rokita, A transient product of DNA alkylation can be stabilized by binding localization, *J. Am. Chem. Soc.*, 2003, **125**, 14005–14013; (b) Q. Zhou and S. E. Rokita, A general strategy for target-promoted alkylation in biological systems, *Proc. Natl. Acad. Sci. U. S. A.*, 2003, **100**, 15452–15457; (c) P. Wang, R. Liu, X. Wu, H. Ma, X. Cao, P. Zhou, J. Zhang, X. Weng, X. L. Zhang, X. Zhou and L. Weng, A potent, water-soluble and photoinducible DNA cross-linking agent, *J. Am. Chem. Soc.*, 2003, **125**, 1116–1117; (d) S. N. Richter, S. Maggi, S. Colloredo Mels, M. Palumbo and M. Freccero, Binol quinone methides as bisalkylating and DNA cross-linking agents, *J. Am. Chem. Soc.*, 2004, **126**, 13973–13979.
- 5 (a) M. Engholm and T. H. Koch, Coupling of the anthracycline antitumor drug menogaril to 2'-deoxyguanosine through reductive activation, *J. Am. Chem. Soc.*, 1989, **111**, 8291–8293; (b) G. Gaudiano, M. Frigerio, P. Bravo and T. H. Koch, Intramolecular trapping of the quinone methide from reductive cleavage of daunomycin with oxygen and nitrogen nucleophiles, *J. Am. Chem. Soc.*, 1990, **112**, 6704–6709; (c) S. R. Angle and W. Yang, Nucleophilic addition of 2'-deoxynucleosides to the *o*-quinone methides 10-(acetyloxy)- and 10-methoxy-3,4-dihydro-9(2H)-anthracenone, *J. Org. Chem.*, 1992, **57**, 1092–1097; (d) S. R. Angle, J. D. Rainer and C. Woytowicz, Synthesis and Chemistry of Quinone Methide Models for the Anthracycline Antitumor Antibiotics, *J. Org. Chem.*, 1997, **62**, 5884–5892.
- 6 (a) D. Verga, M. Nadai, F. Doria, C. Percivalle, M. Di Antonio, M. Palumbo, S. N. Richter and M. Freccero, Photogeneration and reactivity of naphthoquinone methides as purine selective DNA alkylating agents, *J. Am. Chem. Soc.*, 2010, **132**, 14625–14637; (b) F. Doria, S. N. Richter, M. Nadai, S. Colloredo-Mels, M. Mella, M. Palumbo and M. Freccero, BINOL-amino acids conjugates as triggerable carriers of DNA-targeted photocytotoxic agents, *J. Med. Chem.*, 2007, **50**, 6570–6579.
- 7 D. A. Bolon, Stevens rearrangements of N,N,N-trimethylneopentylammonium iodide, *J. Org. Chem.*, 1970, **35**, 3666–3670.
- 8 (a) G. G.-H. Qiao, K. Lenghaus, D. H. Solomon, A. Reisinger, I. Bytheway and C. Wenstrup, 4,6-Dimethyl-*o*-quinone Methide and 4,6-Dimethylbenzoxete, *J. Org. Chem.*, 1998, **63**, 9806–9811; (b) E. Dorrestijn, M. Kranenburg, M. V. Ciriano and P. Mulder, The Reactivity of *o*-Hydroxybenzyl Alcohol and Derivatives in Solution at Elevated Temperatures, *J. Org. Chem.*, 1999, **64**, 3012–3018; (c) M. Yato, T. Ohwada and K. Shudo, 4H-1,2-Benzoxazines as novel precursors of *o*-benzoquinone methide, *J. Am. Chem. Soc.*, 1990, **112**, 5341–5342.
- 9 P. Pande, J. Shearer, J. Yang, W. A. Greenberg and S. E. Rokita, Alkylation of Nucleic Acids by a Model Quinone Methide, *J. Am. Chem. Soc.*, 1999, **121**, 6773–6779.
- 10 R. W. Van De Water and T. R. R. Pettus, *o*-Quinone methides: intermediates underdeveloped and underutilized in organic synthesis, *Tetrahedron*, 2002, **58**, 5367–5405.
- 11 P. Wan, B. Barker, L. Diao, M. Fisher, Y. Shi and C. Yang, Quinone methides: relevant intermediates in organic chemistry, *Can. J. Chem.*, 1996, **74**, 465–475.
- 12 (a) P. Wan and B. Chak, Structure–reactivity studies and catalytic effects in the photosolvolysis of methoxy-substituted benzyl alcohols, *J. Chem. Soc., Perkin Trans. 2*, 1986, 1751–1756; (b) L. Diao, C. Yang and P. Wan, Quinone methide intermediates from the photolysis of hydroxybenzyl alcohols in aqueous solution, *J. Am. Chem. Soc.*, 1995, **117**, 5369–5370.
- 13 (a) Y. Chiang, A. J. Kresge and Y. Zhu, Kinetics and mechanism of hydration of *o*-quinone methides in aqueous solution, *J. Am. Chem. Soc.*, 2000, **122**, 9854–9855; (b) Y. Chiang, A. J. Kresge and Y. Zhu, Flash photolytic generation of ortho-quinone methide in aqueous solution and study of its chemistry in that medium, *J. Am. Chem. Soc.*, 2001, **123**, 8089–8094; (c) Y. Chiang, A. J. Kresge and Y. Zhu, Flash photolytic generation of *o*-quinone α -phenylmethide and *o*-quinone α -(*p*-anisyl) methide in aqueous solution and investigation of their reactions in that medium, saturation of acid-catalyzed hydration, *J. Am. Chem. Soc.*, 2002, **124**, 717–722; (d) Y. Chiang, A. J. Kresge and Y. Zhu, Flash photolytic generation of *p*-quinone methide in aqueous solution. An estimate of rate equilibrium for heterolysis of the carbon-bromine bond in *p*-hydroxybenzyl bromide, *J. Am. Chem. Soc.*, 2002, **124**, 6349–6356.
- 14 K. Nakatani, N. Higashida and I. Saito, Highly efficient photochemical generation of *o*-quinone methide Mannich bases of phenol derivatives, *Tetrahedron Lett.*, 1997, **38**, 5005–5008.
- 15 N. Basarić, I. Žabčić, K. Mlinarić-Majerski and P. Wan, Photochemical formation and chemistry of long-lived adamantylidene quinone methides and 2-adamantyl cations, *J. Org. Chem.*, 2010, **75**, 102–116.
- 16 M. Di Antonio, F. Doria, S. N. Richter, C. Bertipaglia, M. Mella, C. Sissi, M. Palumbo and M. Freccero, Quinone methides tethered to naphthalene diimides as selective G-quadruplex alkylating agents, *J. Am. Chem. Soc.*, 2009, **131**, 13132–13141.
- 17 N. Basarić, N. Cindro, Y. Hou, I. Žabčić, K. Mlinarić-Majerski and P. Wan, Competing photodehydration and excited-state intramolecular proton transfer (ESIPT) in adamantly derivatives of 2-phenylphenol, *Can. J. Chem.*, 2011, **89**, 221–234.
- 18 R. N. Mirrington and G. I. Feutrill, Ornicol monomethyl ether, *Org. Synth.*, 1973, **53**, 90–94.
- 19 (a) D. W. Brusmiche, M. Xu, M. Lukeman and P. Wan, Photohydration and photosolvolysis of biphenyl alkenes and alcohols via biphenyl quinone methide-type intermediates and diarylmethyl carbocations, *J. Am. Chem. Soc.*, 2003, **125**, 12961–12970; (b) Y. Shi and P. Wan, Solvolysis and ring closure of quinone methides photogenerated from biaryl systems, *Can. J. Chem.*, 2005, **83**, 1306–1323; (c) M. Xu, M. Lukeman and P. Wan, Photogeneration and chemistry of biphenyl quinone methide from hydroxybiphenyl methanols, *Photochem. Photobiol.*, 2006, **82**, 50–56; (d) L. Diao and P. Wan, Chemistry of photogenerated α -phenyl-substituted *o*-, *m*-, and *p*-quinone methides from phenol derivatives in aqueous solution, *Can. J. Chem.*, 2008, **86**, 105–118; (e) M. Xu, C. Z. Chen and P. Wan, Intramolecular charge transfer in photoexcited hydroxyterphenyls: Evidence for formation of terphenyl quinone methides in aqueous solution, *J. Photochem. Photobiol., A*, 2008, **198**, 26–33; (f) N. Behin Aein and P. Wan, Excited state intramolecular proton transfer (ESIPT) from phenol OH (OD) to adjacent “aromatic” carbons in simple biphenyls, *J. Photochem. Photobiol., A*, 2009, **208**, 42–49.
- 20 (a) J. Lee, G. W. Robinson, S. P. Webb, L. A. Philips and J. H. Clark, Hydration dynamics of protons from photon initiated acids, *J. Am. Chem. Soc.*, 1986, **108**, 6538–6542; (b) G. W. Robinson, Proton charge transfer involving the water solvent, *J. Phys. Chem.*, 1991, **95**, 10386–10391; (c) L. M. Tolbert and J. E. Haubrich, Photoexcited proton transfer from enhanced photoacids, *J. Am. Chem. Soc.*, 1994, **116**, 10593–10600; (d) K. M. Solntsev, D. Huppert, N. Agmon and L. M. Tolbert, Photochemistry of “super” photoacids. 2. Excited-state proton transfer in methanol/water mixtures, *J. Phys. Chem. A*, 2000, **104**, 4658–4669.
- 21 H. J. Kuhn, S. E. Braslavsky and R. Schmidt, Chemical actinometry, *Pure Appl. Chem.*, 2004, **76**, 2105–2146.
- 22 (a) H. E. Zimmermann and V. R. Sandel, Mechanistic organic photochemistry. II. solvolytic photochemical reactions, *J. Am. Chem. Soc.*, 1963, **85**, 915–922; (b) H. E. Zimmermann, The meta effect in organic photochemistry: Mechanistic and exploratory organic photochemistry, *J. Am. Chem. Soc.*, 1995, **117**, 8988–8991.
- 23 M. Lukeman and P. Wan, A new type of excited-state intramolecular proton transfer: Proton transfer from phenol OH to a carbon atom of an aromatic ring observed for 2-phenylphenol, *J. Am. Chem. Soc.*, 2002, **124**, 9458–9464.
- 24 Y. Shi and P. Wan, Charge polarization in photoexcited alkoxy-substituted biphenyls: Formation of biphenyl quinone methides, *J. Chem. Soc., Chem. Commun.*, 1995, 1217–1218.
- 25 M. Montalti, A. Credi, L. Prodi and M. T. Gandolfi, *Handbook of Photochemistry*, CRC Taylor and Francis, Boca Raton, 2006.
- 26 (a) M. Fisher and P. Wan, Nonlinear solvent water effects in the excited-state (formal) intramolecular proton transfer (ESIPT) in *m*-hydroxy-1,1-diaryl alkenes: Efficient formation of *m*-quinone methides, *J. Am. Chem. Soc.*, 1999, **121**, 4555–4562; (b) L. M. Tolbert and K. M. Solntsev, Excited-state proton transfer: From constrained systems to “super” photoacids to superfast proton transfer, *Acc. Chem. Res.*, 2002, **35**, 19–27; (c) N. Agmon, Elementary Steps in Excited-State Proton Transfer, *J. Phys. Chem. A*, 2005, **109**, 13–35.
- 27 R. Townsend and S. G. Schulman, Acidity of hydroxybiphenyls in the lowest excited singlet state: The influence of substituent orientation, *Chim. Oggi*, 1992, **10**, 49–52.
- 28 L. J. Johnston and N. P. Schepp, Laser flash photolysis studies of the reactivity of styrene radical cations, *Pure Appl. Chem.*, 1995, **67**, 71–78.
- 29 P. R. Levin, I. V. Khudyakov, V. A. Kuz'min, H. J. Hageman and C. R. H. I. de Jonge, Flash photolysis study of phenyl-substituted phenols,

- quinones and corresponding free radicals. Part 3. Intermediates in the photolysis of phenyl-substituted phenols, *J. Chem. Soc., Perkin Trans. I*, 1981, 1237–1239.
- 30 (a) R. A. McClelland, C. Chan, F. L. Cozens, A. Modro and S. Steenken, Laser flash photolysis generation, spectra, and lifetimes of phenylcarbenium ions in trifluoroethanol and hexafluoroisopropyl alcohol. On the UV spectrum of the benzyl cation, *Angew. Chem., Int. Ed. Engl.*, 1991, **30**, 1337–1339; (b) F. L. Cozens, V. M. Kanagasabapathy, R. A. McClelland and S. Steenken, Lifetimes and UV-visible absorption spectra of benzyl, phenethyl, and cumyl carbocations and corresponding vinyl cations. A laser flash photolysis study, *Can. J. Chem.*, 1999, **77**, 2069–2082.
- 31 R. A. McClelland, V. M. Kanagasabapathy, N. S. Banait and S. Steenken, Flash-photolysis generation and reactivities of triarylmethyl and diarylmethyl cations in aqueous solutions, *J. Am. Chem. Soc.*, 1989, **111**, 3966–3972.
- 32 R. A. McClelland, V. M. Kanagasabapathy, N. S. Banait and S. Steenken, Reactivities of triarylmethyl and diarylmethyl cations with azide ion investigated by laser flash photolysis. Diffusion-controlled reactions, *J. Am. Chem. Soc.*, 1991, **113**, 1009–1014.
- 33 J. A. Pincock, The Photochemistry of Substituted Benzenes: Photo-transpositions and the Photoadditions of Alcohols, in *CRC Handbook of Organic Photochemistry and Photobiology*, ed. W. M. Horspool, F. Lenci, CRC Press LLC, Boca Raton, FL, 2004, 2nd edn, Ch. 46, pp. 1–19.
- 34 L. C. Anderson and W. A. Fisher, Quinoidation of triaryl compounds-hydroxybiphenyldiarylmethyl cations, *J. Am. Chem. Soc.*, 1944, **66**, 594–597.
- 35 T. Inukia, Rates of solvolysis of substituted 4-biphenyldimethylcarbinyl chlorides: A test of the free-energy relationship, *Bull. Chem. Soc. Jpn.*, 1962, **35**, 400–407.
- 36 H. R. Sullivan, R. E. McMahon, P. Roffey, D. G. Hoffman, F. J. Marshall, R. E. Billings, D. N. Benslay and W. S. Marshall, Isopropylbiphenyl metabolism in the rat. Relationships between metabolism, pharmacology and toxicology, *Xenobiotica*, 1978, **8**, 333–240.
- 37 T. Tanigaki, *Ger. Offen.*, 3402831, 09 August 1984.
- 38 T. Mossman, Rapid colorimetric assay for cellular growth and survival: Application to proliferation and cytotoxicity assays, *J. Immunol. Meth.*, 1983, **65**, 5563.
- 39 M. R. Boyd and D. P. Kenneth, Some practical considerations and applications of the National Cancer Institute in vitro anticancer drug discovery screen, *Drug Dev. Res.*, 1995, **34**, 91–109.